INTERNATIONAL SOCIETY FOR SOIL MECHANICS AND GEOTECHNICAL ENGINEERING

The Ninth James K. Mitchell Lecture: On The Geomechanics and Geocharacterization of Tailings

Fernando Schnaid

Federal University of Rio Grande do Sul (UFRGS), Graduate Program in Civil Engineering (PPGEC/UFRGS), Porto Alegre, Brazil, fschnaid@gmail.com

ABSTRACT: The prediction of the short and long-term properties of silty and sandy tailings is among the greatest geotechnical and geoenvironmental challenges of our time. Governed by flow and cyclic liquefaction, the engineering characteristics of tailings under shear are dictated by the development of large strains, accompanied by increases in pore pressures and reduction in deviatory and mean stresses. This phenomenon can be described under the concepts of Critical State Soil Mechanics by modelling some specific aspects of behaviour such as the unstable strain-softening response and the shape of the critical state line. In situ tests can only be interpreted with reference to this framework. In addition, it is recognized that, as intermediate permeability materials, in situ test results can only be analysed after full account for the drainage effects taking place during shearing. All these aspects are reviewed in this paper and guidance for industry is provided on the theoretical background and techniques required to maintain mineral supplies while reducing catastrophic failures, loss of lives and environmental consequences of mining extraction. It is acknowledged that industry funding along with government support were critical to the development of the present work.

Keywords: tailings dams; static liquefaction; critical state soil mechanics; *in situ* tests

1. Introduction

The mining industry supplies the necessary metals and minerals that make modern life sustainable. A central role for low carbon future, the ever-increasing need for extraction and production of mineral confront professionals with environmental, economic and social challenges originated from the mining industry and, specially, from the disposal of mining tailings.

Tailings are stored in the form of piles as dry stacks, hydraulically deposited in tailings dams and placed underground in

excavated galleries or in open pits as backfills. All these storage structures are referred to as Tailings Storage Facilities (TSF). For the case of tailings dams, they are among the largest geotechnical structures ever constructed. Showing high probability of structural failure, tailings impoundments are complex man-made systems that, by their own nature, have intrinsic geomechanics design challenges emerging from flow and cyclic liquefaction. Consequences of tailings failure liquefaction are massive mudslides, followed by fast-moving mudflows, causing disastrous humanitarian and environmental consequences.

Gens (2019) listed examples of landmark cases reporting foundation and flow liquefaction failures of tailings dams including Stava Fluorite Mine (1985) in Italy (Chandler and Tosatti, 1995), Sullivan Mine (1991) in Canada (Davies et al. 2002), Merriespruit Harmony Mine (1994) in South Africa (Fourie et al. 2001), Aznalcóllar Tailings Dam (1997) in Spain (Gens and Alonso, 2006), Mount Polley Dam (2014) in Canada (Morgenstern et al, 2015), Fundão Dam (2015) in Brazil (Morgenstern et al, 2016) and Brumadinho Dam (2019) also in Brazil (Robertson et al, 2019). The recent accidents of Mount Polley, Fundão and Brumadinho show that unsafe conditions are not easily perceived, mine waste materials may perform worse than expected,

and time-delayed triggering mechanisms cannot be disregarded.

Images of the Brumadinho Dam before and after failure are shown in Fig. 1. The Report of the Expert Panel on the Technical Causes of the Failure (Robertson et al., 2019) provided insights as to the reasons for the 2019 catastrophic failure. The dam was constructed using the upstream construction method over a period of 37 years in 10 raises. No new raisings were constructed after 2013, and tailings disposal ceased in July 2016. The material in the dam showed a sudden and significant loss of strength and rapidly became a heavy liquid that flowed downstream at a high speed as the result of flow (static) liquefaction. The failure extended across much of the face of the dam and collapse of the slope was complete in less than 10 seconds, with 9.7 Mm3 of material (representing approximately 75 percent (%) of the stored tailings) flowing out of the dam in less than 5 minutes.

The historical CPTu data indicated that the tailings were predominately loose, saturated, and contractive at large strains. Advanced laboratory testing on representative reconstituted samples of the tailings showed brittle strength loss behaviour and indicated the presence of bonding which was attributed to iron oxidation. The bonding rendered the tailings stiff and potentially brittle which may explain the lack of observable deformations prior to failure and the sudden, rapid response at failure. The Panel concluded that the sudden strength loss and resulting failure of the marginally stable dam were due to a critical combination of ongoing internal strains due to creep, and a strength reduction due to loss of suction in the unsaturated zone caused by the intense rainfall towards the end of 2018.

An inquiry led by mining industry investors in 2019 (Mining and Tailings Safety Initiative), in response to the Brumadinho disaster in Brazil, has found that 10% of tailings dams exhibited stability problems in their lifetime. This investigation reports a cumulative 45 billion cubic meters of tailings currently storaged

worldwide in 1,700 tailings dams. Other sources report 9,000 tailings dams in operation or decommissioned. In this global scenario, tailings dam failures of significant scale from the last decade are examples of constructed works that did not perform under designed conditions, with accidents often occurring in developed countries and in first class mining corporations.

.

a)   Before failure, looking North.

b)   6 min. after the first observed deformation
Figure 1. Brumadinho Dam failure (Robertson et al., 2019).

It has also been reported that although the severe failure rate per million tonnes of ore production is decreasing, the safety improvements have not prevented the serious and very serious TSF failures to increase over the last century, a period in which more than 30 major accidents have been reported and the resulting fast-moving mudflows have led to a cumulative loss of almost 3000 lives (Fig. 2). As a consequence, liquefaction of the impoundment material is forcing regulators and industry to question international standard guidelines of tailings dams design. Prof. Morgenstern (2019) stated in his 2019 Victor de Mello Lecture: "At this time, there is a crisis associated with concern over the safety of tailings dams and lack of trust in their design and performance."

To respond to the needs of society towards preventing dam failures, the first and essential step is to examine the fundamental behaviour of tailings, develop new technologies and procedures for better characterizing tailings impoundments, anticipate their potential for liquefaction, and predict their corresponding constitutive parameters. This 9th J.K. Mitchell Lecture gives the opportunity to peer review of these research topics to better understand the complex behaviour of tailings. Experience on tailings such as iron, gold, bauxite and zinc is reported and key aspects of behaviour that are relevant to the design of TSF are addressed. Special attention is given to geotechnical characterization of tailings, focusing on the interpretation of *in situ* tests and susceptibility to flow liquefaction. It attempts to complement previous important contributions in this

field (e.g. Castro, 1969; Mitchell, 1976; Ishihara, 1993; Jamiolkowski, 2013; Jefferies and Been, 2016, among many others).
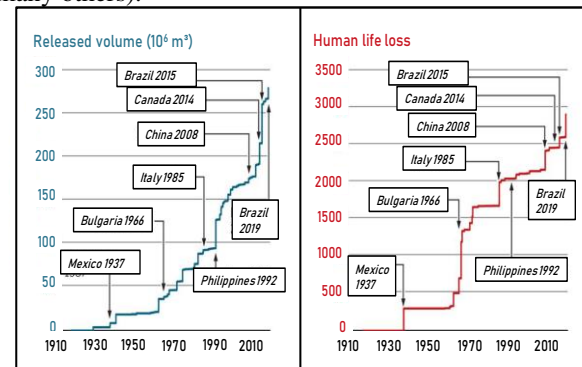
Figure 2. Released volume and life loss due to catastrophic tailings and ash-pond dams (Santamarina et al, 2019).

2. Basic geomechanical behaviour of granular tailings

Tailings are the by-product of extractive industries that crush and grind rocks for extraction of economic minerals. Hydraulically deposited, mine tailings show considerable spatial variability of their physical and mineralogical properties, with variable gradings and particle morphologies due to processing of rocks that are heterogeneous in nature and the actual deposition processes. The approach developed herein focus on tailings consisting of non-plastic sand, silt and clay-sized particles, without clay minerals, that exhibit little physicochemical activities. The diagenesis of these sediments can often be disregarded, because particles are relatively inert and their characteristics are determined primarily by particle size, shape, surface texture, and size distribution (Mitchell, 1976; Mitchell and Soga, 2005).

In addition, it is recalled that as recently deposited materials, tailings exhibit normally-consolidated states. However, the importance of microstructure (aging and/or cementation) on properties of tailings cannot be always disregarded which implies that, at a given void ratio, some tailings can sustain stresses higher than could the same material non-microstructured. Evidences of microstructure in tailings where reported by Robertson (2016) and endorsed by the fact that Brumadinho tailings had light cementation (bonding) that had a significant impact on behaviour (Robertson et al., 2019). Measurements from the small strain shear modulus provide solid indication of tailings microstructure, because bonding and aging reinforces the links between particles, and so increases the small strain shear modulus, even at the same void ratio (e.g. Robertson, 2016; Schnaid et al, 2020). Conversely, microstructure at small strains bears no relation to the microstructure effects on large deformation strength and these effects are not easily perceived.

With due recognition of the complex nature of tailings, key aspects of their geomechanical behaviour can be described under the concepts of Critical State Soil Mechanics. Tested tailings show a unique critical state line (CSL), but a notable characteristic feature of tailings is that the CSL often exhibits a marked curvature dictated by transitions of state (e.g., Been et al. 1991; Verdugo

and Ishihara 1996; Carrera et al., 2011; Bedin et al.; 2012; Schnaid et al., 2013). The slope of the CSL becomes flatter at low mean stresses, with the undrained shear strength reducing continuously, leading ultimately to true liquefaction at low stress levels. In these cases, tailings will not sustain a constant value of deviatory stress leading to high strain softening and subsequent failure by flow liquefaction. As the mean stress increases, samples may still develop strain-softening, with high compressibility, that will gradually evolve to strain-hardening. Additionally, the curvature of a CSL at high stresses is caused by the onset of the particle breakage (e.g. Lade, 1992; Konrad 1998, Bedin et al.; 2012; Schnaid et al, 2013).

This behaviour is illustrated by the results of triaxial compression and extension tests in gold tailings reported by Schnaid et al, (2013; 2019). Testes carried out under both drained and undrained stress paths are shown in Fig.

3, represented in the $p' - q$ and $e - lnp'$ spaces (being p' the mean effective stress, q the deviatoric stress and e the void ratio). Tests with confining pressures above 200kPa denote an undrained behaviour with stability reflected by strain-hardening. For lower confinement stresses the undrained response of loose specimens exhibit strong strain softening response, with some intermediate points (σ'_c= 50 – 200 kPa) reaching still a positive shear strength (with no drop to zero), while for the range of σ'_c= 0 – 50 kPa the strain softening is followed by a complete loss of stability. In this range, there is a rapid increase in shear strains and uncontrolled pore pressure development. Positive pore water pressure in shear was observed in all tests revealing the tendency to contractive response of gold tailings, which at low pressure may lead to liquefaction, a tendency that is gradually suppressed as the confining pressure increases.
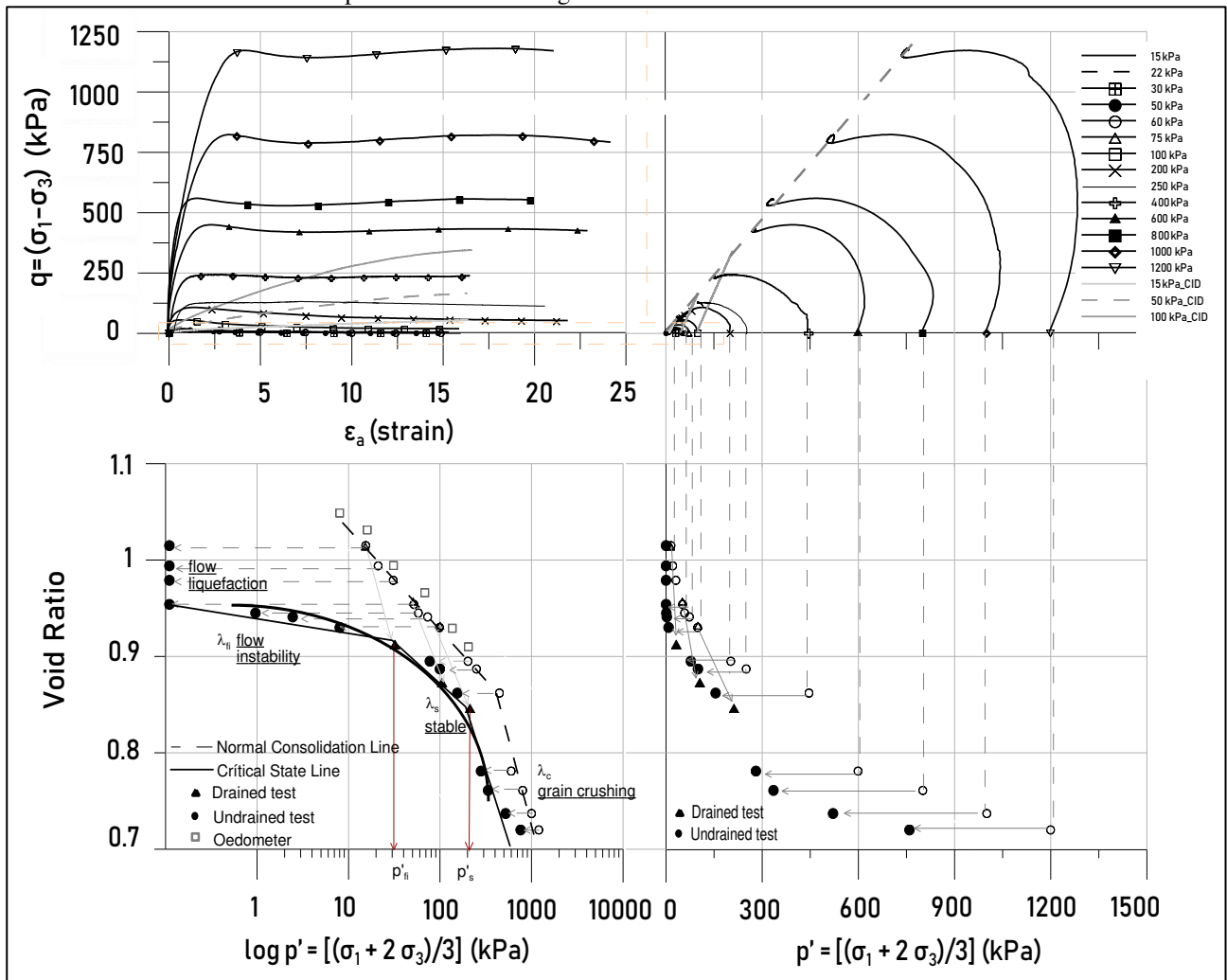

Figure 3. Triaxial compression tests (after Schnaid et al, 2013).

Figure 4 summarizes the CSLs of different tailings (Li et al, 2018). Except for the iron tailings reported by Li and Coop (2019), all the CSLs are curved, and are fairly flat at low to medium stresses but tending to be parallel to their corresponding NCL at high stresses. Importantly, the horizontal asymptote of the CSL controls full static liquefaction, although strong strain softening behaviour will still take place for undrained tests that reach the curved section of the CSL.

The importance of advanced constitutive models representing the characteristic features associated to the mechanical behaviour of tailings is essential to geotechnical design. More than 30 constitutive models have been developed for sands, some of which have already adopted non-linear equations to express the shape of the critical state line (e.g. Li and Wang, 1998; Pestana and Whittle, 1999; Dafalias and Manzari, 2004, 2008; Taborda et al, 2004; Loukidis and Salgado, 2009;

Jefferies and Been, 2016), but few have been encoded in software package tools used routinely in geotechnical practice.

For example, in NorSand (Jefferies and Been, 2016), the critical state locus has been defined by two models:

Conventional CSL Idealization (semi-log linear):

$$e_c = \Gamma - \lambda_{10} log\ (p'_c) \tag{1}$$

Improved CSL Idealization (curved):

$$e_c = a + b\left(\frac{p'_c}{p'_{ref}}\right)^{\alpha} \tag{2}$$

where e_c is the critical void ratio, Γ is the void ratio at the critical state at reference pressure of 1 kPa, p' is the mean effective stress, and λ_{10} is the slope of the CSL in a semi-logarithm space [$e\ vs.\ log\ (p')$]. The parameters a, b, and α are fitted to match test results, and p'_{ref} is taken as 1atm (101.32 kPa).
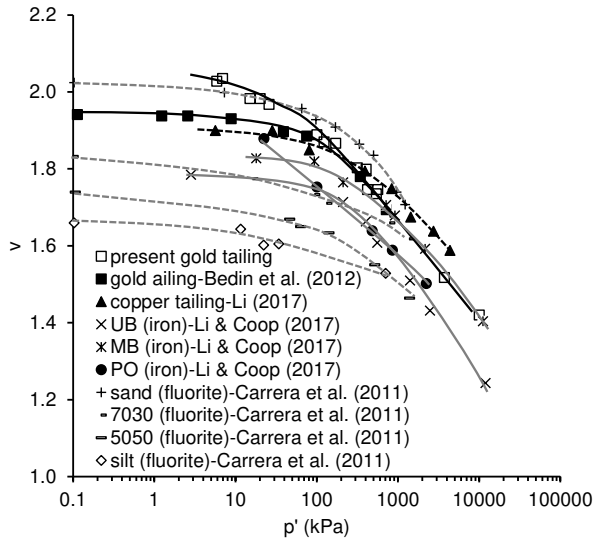

Figure 4. The CSLs of different tailings (Li et al, 2018).

These concepts describe the essence of the flow liquefaction mechanism, as already outlined in early works from Castro (1969), NRC (1985), Kramer (1996), Yoshimine and Ishihara, 1998; Lade, 1999; Li and Dafalias, 2000; Andrade (2009), Jefferies and Been (2016), and others. In line with these classical references, flow instability is defined as a phenomenon that triggers the development of large strains, corresponding to a strain-softening behaviour accompanied by increasing pore pressures and a reduction in deviatory stresses. Only in extreme conditions does the increase in pore pressures lead to a complete loss in shear strength, with samples experiencing very large strains and reaching a true liquefaction state, i.e., complete loss of effective stresses. Flow liquefaction of slopes, embankments, or foundations of tailings dams occurs when undrained strain softening is triggered by either static loading or by deformation under a static shear stress, reaching a condition in which the shear stress required for the soil mass to reach static equilibrium is greater than the shear strength of the soil in its residual (liquefiable) state.

In addition, loose saturated low and non-plastic soils and tailings tend to contract when subjected to cyclic loading triggered by the ground motions associated with earthquakes or vibrations such as those generated from pile driving, heavy earthmoving equipment, rotating machinery and mine explosions. The cyclic responses and strength of soils and tailings, represented by the cyclic strength (resistance) ratio CRR can be measured in the laboratory. Constant volume cyclic simple shear tests or cyclic triaxial tests can be conducted to determine the cyclic shear resistance of undisturbed and reconstituted soils and tailings samples at various densities and confining stresses. The procedures for cyclic laboratory-based liquefaction resistance testing are summarized in Idriss and Boulanger (2004).

As we seek to discuss certain design problems, it is worth recalling that data reported in the literature in materials exhibiting high potential for liquefaction have been interpreted using critical state soil mechanics as the background, often gathered from samples reconstituted in the laboratory at the in situ voids ratio, given the difficulty in retrieving undisturbed samples. In clays, retrieving undisturbed samples has become the standard of practice where drive sampling or block sampling techniques are well developed, and sample quality can be readily assessed. On the other hand, the shortcomings of sampling silts are well recognized, and "undisturbed" samples can only be obtained and handled by sophisticated and expensive processes such as the gel push sampler or block sampler (e.g. Jamiolkowski, 2013; Jamiolkowski and Masella, 2015; Viana de Fonseca et al., 2019). Even when using these techniques, disturbance of the sample may not be completely eliminated and retrieving high-quality, undisturbed samples remains a challenge. Besides, it is assumed that the critical and steady state lines are equivalent, without discussing the formalism behind the development of these theoretical frameworks.

Without undisturbed samples, dam analysis and design using lab-measured soil properties becomes inaccurate. Engineers have then to rely on preparing reconstituted representative samples by dry or wet pluviation, slurry deposition, vibrations, or moist tamping (e.g. Ladd, 1997). Each one of these laboratory specimen preparation procedures produces a distinct soil fabric that does not necessarily represent the in-situ properties and may not replicate the potential collapse fabric of water-deposited grains (e.g. Vaid et al, 1995; Hoeg et al, 2000; Lerouiel and Hight, 2003, Li et al, 2018). Consequences are that laboratory element testing on reconstituted samples is only useful in determining material properties at critical state, after all particle orientation has reached a steady state condition. Linking the critical state conditions measured in the laboratory with the ground state conditions requires support of in situ testing techniques.

3. Interpretation of in situ testing

Interpretation of in situ tests in silts has been historically based on empirical approaches, developed from experience and supported by case-study database. Empirically based recommendations offer sound support for the assessment of soil properties in ground conditions which are known from comparable experience, but may

produce inconsistent characterization when extrapolated to other environments, such as in the case of tailings. In addition, it is recalled that interpretation of in situ tests applies only for granular materials that are not microstructured.

The most used field investigation techniques are the piezocone penetration test (CPTU) and the standard penetration test (SPT), accompanied by field vane test (FVT), dilatometer (DMT) and self-boring pressuremeter (SBP). For these tests, current and future best practices guidance for investigation should be rooted on four fundamental principles:

1. Acquire background information from site geology, hydrogeology, dam construction and operation history to assist on the interpretation of measured testing data.

2. Avoid resorting to empirical adjustment factors when interpreting testing data by framing the interpretation into the concepts of critical state soil mechanics.

3. Integrate measurements from advanced field and laboratory experiments to enhance the ability in describing and modelling the complex geomechanical behaviour of tailings.

4. Be aware that in intermediate permeability tailings, often referred to as transitional materials, interpretation of field tests requires assessing partial drainage effects within the soil surrounding the testing device.

In intermediate permeability tailings, drainage conditions affect the interpretation of in situ test results. If partially drained conditions prevail it may be necessary to change the rate of shearing to control the drainage conditions developed during the test, imposing either drained or undrained conditions. So, to start with, the influence of rate effects controlling measurements of in situ tests must be given careful consideration.

4. In situ test rate effects

The influence of factors affecting the shear rate of in situ tests has been a subject of numerous recent publications, which have elucidated important aspects related to uncertainties in pore pressure measurements and the associated errors in estimating the coefficient of consolidation and the undrained shear strength in intermediate permeability soils. This is a relevant topic in mining tailings, because the hydraulic disposal process often produces silt-particle materials with permeability ranging from $10^{-5} < k < 10^{-8}$ m/s, where the standardized testing rate adopted in geotechnical investigation may lead to partial drainage and, thus, erroneous estimation of undrained parameters.

Identification of partial drainage effects occurring during in situ tests is made by accounting for probe size, testing rates and soil consolidation characteristics, which are evaluated in the form of dimensionless groups of relevant parameters and defined as normalized velocity:

$$V_h = v_d/c_h \text{ or } V_v = v_d/c_v \tag{3}$$

$$\overline{Vh} = \frac{v \cdot t_{50}}{d \cdot \sqrt[4]{Ir}} \tag{4}$$

$$V_h = v/k \tag{5}$$

where v is the testing velocity, d is the probe diameter, c_h (or c_v) is the coefficient of consolidation and k is the coefficient of hydraulic conductivity.

Departing from concepts that govern pore-fluid pressure diffusion in a linear poroelastic medium, (e.g. Coussy, 2004; Dormieux et al, 2006), Randolph and Hope (2004) introduced the normalized penetration velocity $V = v/v_c$ for CPTU interpretation outlined in Eq. (3) that was defined according to vertical drainage conditions and later extended to radial drainage. Although Eq. (3) captures the key elements which need to be considered for in situ testing interpretation, uncertainties on how to apply the method in engineering practice have been recognized. Since penetration in silts is not fully undrained, the value of t_{50}^* estimated using the piezocone under-predicts the value actually measured after some consolidation and needs correction before calculating V_h (DeJong and Randolph, 2012). Instead, an alternative approach defined in Eq. (4) stems from the heuristic idea that a characteristic value for V_h might be evaluated in intermediate permeability soils by simply expressing the velocity factor as a function of t_{50}^* only (Schnaid et al, 2019). Alternatively, a simplified expression for fixed probe dimensions can be used for any in situ testing tool (Eq. 5). All forms of normalization embrace the same variables and will be used later to (a) demonstrate that normalization of shear velocity is an important factor in assessing soil properties and (b) for comparative performance of data from different geomaterials.

Application of normalization principles to in situ testing interpretation are reported for CPTU penetration testing (e.g. Randolph and Hope, 2004), vane torsion (Blight, 1968, Dienstmann et al, 2018) and DMT expansion tests (Schnaid et al., 2016; 2018).

In practice, two alternative approaches may be considered when using the normalized velocity concept: (a) select appropriate testing rates to ensure that either fully drained or fully undrained shear conditions are achieved or (b) for standard testing rates, correct in situ measurements to account for the possible errors induced by pore pressure dissipation. The first approach stems from a practical recommendation of performing tests at different rates, selecting appropriate non-standard testing rates to avoid partial drainage. The second approach works as an alternative to correct data recorded at standard testing rates (tested according to International Reference Test Procedures). This later approach discussed herein needs scientific scrutiny and experimental validation.

4.1. Piezocone CPTU tests

Cone penetration is the most accepted and used in situ test to obtain a continuous stratigraphic profile, and to estimate the engineering parameters of tailings. In the intermediate permeability range, rate effects are evaluated in the normalized penetration space

represented either by penetration resistance or penetration pore pressures plotted against normalized penetration velocity $V_h(= vd/c_h)$. This space has been successfully used for the data analysis of various penetration tests, indicating that fully undrained penetration typically occurs when V_h is larger than about 50 to100 and fully drained penetration occurs when V_h is less than about 0.01.

A summary of results comparing experimental studies on cone rate dependence is shown in Figure 5, in which the normalized resistance $Q = q_{t,net}/\sigma'_{v0}$ is plotted against the normalized velocity. The database comprise tests performed in centrifuge (Randolph and Hope, 2004; Jaeger et al., 2010; Suzuki et al., 2014), calibration chamber (Kim et al., 2008) and field tests (Suzuki and Lehane, 2014; Dienstmann et al, 2018). A simple observation of reported data shows that the influence of partial consolidation on cone resistance is significant in all soils, especially for normalized velocities V_h ranging from 0.01 to 10. The drained to undrained Q_D/Q_{UD} ratio ranges from 3 to 10, being of the order of 10 in gold and bauxite tailings (Dienstmann et al, 2018). The measured

Q_D/Q_{UD} ratio reflects amount of pore pressure generated during undrained shear controlled by the tendency for volume contraction dictated by the material shear resistance and shear stiffness.

Under drained loading, tailings exhibit strain-hardening response and mobilizes their full angle of shearing resistance at failure. In turn, under undrained loading, tailings behaviour turns to strain-softening and the mobilized peak resistance is much lower than the corresponding peak drained value (e.g. Bedin et al.; 2012; Schnaid et al., 2013).

It is worth mentioning that, from a practical standpoint, DeJong and Randolph (2012) and Robertson (2012) had suggested that when the time for 50% dissipation (t_{50}) from the CPTu tests were greater than about 50s, the CPT penetration is essentially undrained.

Later in this paper, a recommendation is made to compare the undrained shear strength calculated from q_t and from u_2, because when S_u from q_t is equivalent to S_u from u_2, the influence of partial drainage is small.
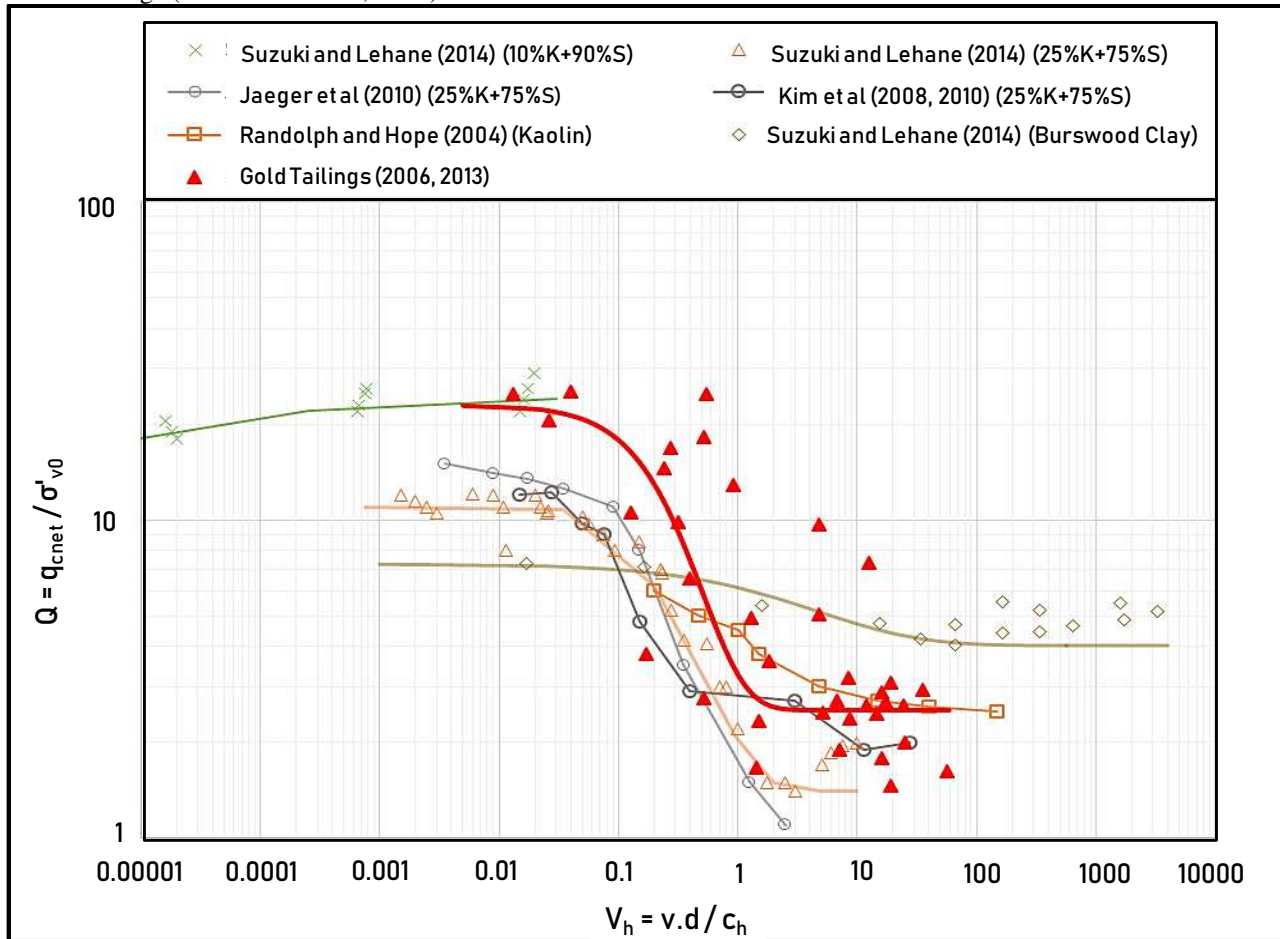
Figure 5. Rate effects in different geomaterials (modified from Suzuki and Lehane, 2014).

Non-standard penetration rates may have to be selected according to local experience from drainage curves established from tests carried out at different velocities and to advanced mathematical models so that the results can be interpreted. Of particular interest is the use of cavity-expansion solutions for modelling cone and pressuremeter tests (e.g Vésic, 1972; Randoph and Wroth, 1979; Baligh, 1985; Teh and Houlsby, 1991; Yu

and Mitchell, 1998, Chen and Abousleiman, 2012; Zhang et al, 2015; among others). Yet, few approaches have been developed to analyse coupled consolidation fields in a saturated porous medium under cylindrical and spherical symmetries (Carter, 1978; Silva et al, 2006; Leclanc and Randolph, 2008; Suryasentana and Lehane, 2014; Dienstmann et al, 2016). From these studies it has been identified that cone penetration resistance can

change significantly with rate effects, which in turn depends on soil compressibility (λ and κ), shear strength (ϕ') and soil consolidation characteristics (c_h).

In assessing the effects of partial drainage, the first step is to quantify the maximum possible error in calculating values of shear strength, which is given by the normalized cone resistance q_{tD}/q_{tUD} assuming undrained penetration (q_{tUD}) for a test that is close to drained conditions (q_{tD}). For simplicity, one can use the framework of traditional bearing capacity theory, based on a rigid-plastic model, derived from the plane strain bearing capacity factor under a number of simplified considerations. Figure 6 presents the normalized cone resistance q_{tD}/q_{tUD} *versus* ϕ' proposed by Senneset et al (1982) and calibrated against recent published data (including tailings). The model predictions show that the values of q_{tD}/q_{tUD} increase with increasing friction angle to values greater than 10 and can be approximated within the $\phi' \in [20°, 50°]$ interval by the following exponential function:

$$\frac{q_{tD}}{q_{tUD}} = 1.57e^{0,04\phi'} \qquad (6)$$

Besides, it is possible to provide guidelines for design by directly correcting the tip cone resistance recorded at the standard penetration rate of 20mm/s (q_{t20}) in order to calculate an equivalent fully undrained penetration resistance, q_{tUD}. In practice, it is necessary to formulate an approximate expression for the ratio q_{t20}/q_{tUD} which, for convenience, is expressed as function of the pore pressure parameter B_q measured at the standard rate of penetration of 20mm/s:

$$\frac{q_{t20}}{q_{tUD}} = 1 + \left(\frac{q_{tD}}{q_{tUD}} - 1\right)\left(\frac{1}{cosh(aB_q{}^b)}\right) \qquad (7)$$

where $B_q = (u_2 - u_0) / (q_t - \sigma_{v0})$ is the pore pressure parameter ratio and a=20 and b=1.5 are fitting parameters.

The difference between drained and undrained strength is due to the amount of pore pressure that can be generated during undrained shear. This is controlled by the tendency for volume contraction that drives the development of excess pore pressure. Hence, the difference is a directly function of soil state, expressed in Eq. 7 by a combination of ϕ' and B_q. The proposed expression should be seen as first approximation supported by experimental data that stands until more rigorous solutions are derived from poromechanical and elasto-plastic models, following recent work by Dienstmann et al. (2017; 2018). For general practical applications in which penetration is not representative of undrained conditions, Eq. (7) allows for correlating the penetration resistance measured at the standard rate of 20mm/s.
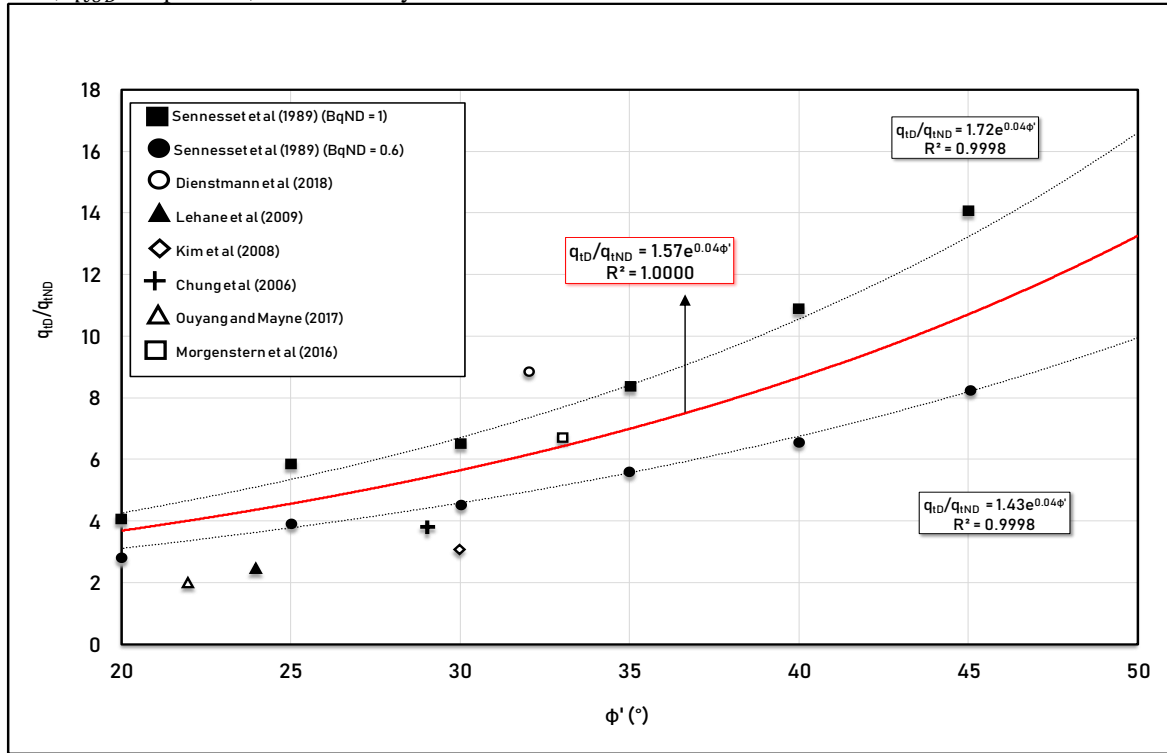

Figure 6. Drained to undrained cone resistance ratio as function of friction angle (modified from Senneset et al., 1982).

4.2. Field Vane Tests (FVT)

It is now generally recognized that the standard rate of vane rotation (0.1 deg/s), yielding a peripheral velocity of 0.057mm/s, ensures undrained conditions of shearing in clays, but may not be applicable to estimate the undrained shear resistance in transitional soils. For vane tests, this would require changing the rate of shearing to control the drainage conditions developed during the test in order to derive constitutive parameters representative of undrained conditions.

Alternatively, it is possible to develop a practical criterion to account for the possible errors induced by pore pressure dissipation based on the manipulation of numerical solutions. Unlike the piezocone, the existing database is incomplete to support empirical correlations.

Most previously reported data related to vane rate effects attempted to evaluate the impact of velocities higher than the standard ($\omega > \omega_{SD} = 0.1$ deg/s) in low permeability materials, thus observing viscous effects on the measured resistance (e.g. Perlow and Richards, 1977; Torstensson, 1977; Biscontin and Pestana, 2001; Peuchen and Mayne, 2007; Schlue et al., 2010).

For capturing the flow effects on the mechanical response of the soil surrounding the rotating cylinder, a simplified model for poromechanical analysis of consolidation induced by the rotation of an infinitely long rigid cylinder embedded within a porous medium was formulated in Dienstmann et al. (2018) and Forcelini at al. (2019). In the model, a rotating rigid cylinder is viewed as a conceptual simplified geometry of the vane test. The model relies on a nonlinear poroelastic stress-strain analysis of soils subjected to shear and compressive stresses, formulated within the Biot's poroelasticity framework for the analysis of the coupled deformation-diffusion process.

The study demonstrated that the ratio between drained and undrained torque T_D/T_{UD} is governed by the soil friction angle. In contrast, stiffness and radius of influence have little effects on changes in this normalized torque. In Figure 7, the results from this analysis are conveniently presented in terms of normalized velocity v/k, where $v = \omega R$ is the linear velocity of the vane. The model predicts T_D/T_{UD} ratios ranging from 1.8 to 2.8, generally lower than 2 and much lower than values calculated for the piezocone. This can be explained by the fact that volumetric strains induced by vane rotation in the drained regime are moderate in comparison to values calculated under cavity expansion (Dientsmann et al., 2018).

For silty soils, the internal friction angle typically ranges from 30^0 to 40^0 corresponding to a narrow interval 0.57-0.84 for $\tan \phi$, which limits the magnitude effects of drainage conditions on measured torque. The variation of T_D/T_{UD} ratio with ϕ' can be approximated within interval $\phi' \in [5°, 45°]$ by the following hyperbolic function:

$$T_D/T_{UD} = \frac{3}{2}\left(1 + \tanh(r_\phi)\right) \qquad with \quad r_\phi = \frac{7}{4}\tan \phi \tag{8}$$

The accuracy of the approximation can be appreciated from Figure 7. In analogy to the interpretation of cone tests, this equation can be used as guideline to assess the maximum error that can be induced by drainage in a vane test.

Referring to the range of internal angle variations, it is also interesting to formulate an approximate expression for the ratio $T_{0.1}/T_{UD}$ between mobilized torque at standard vane velocity ($\omega_{SD} = 0.1$ deg/s) and its counterpart under undrained conditions varying the soil permeability coefficient within range $10^{-9} - 10^{-5}$ m/s:

$$T_{0.1}/T_{UD} = a + b \; \tanh(r_\phi) \quad with \quad r_\phi = \frac{7}{4}\tan \phi \tag{9}$$

where non-dimensional functions a and b depend on the normalized velocity $\bar{v} = v_{SD}/k$. Expressions for these coefficients can be fitted from the numerical solutions obtained from the nonlinear poroelastic modelling as:

$$a = \frac{3 + 0.003 \; \bar{v}}{2 + 0.003 \; \bar{v}}; \quad b = \frac{1.5}{1 + \left(\frac{1}{9}ln(1+\bar{v})\right)^{10}} \tag{10}$$
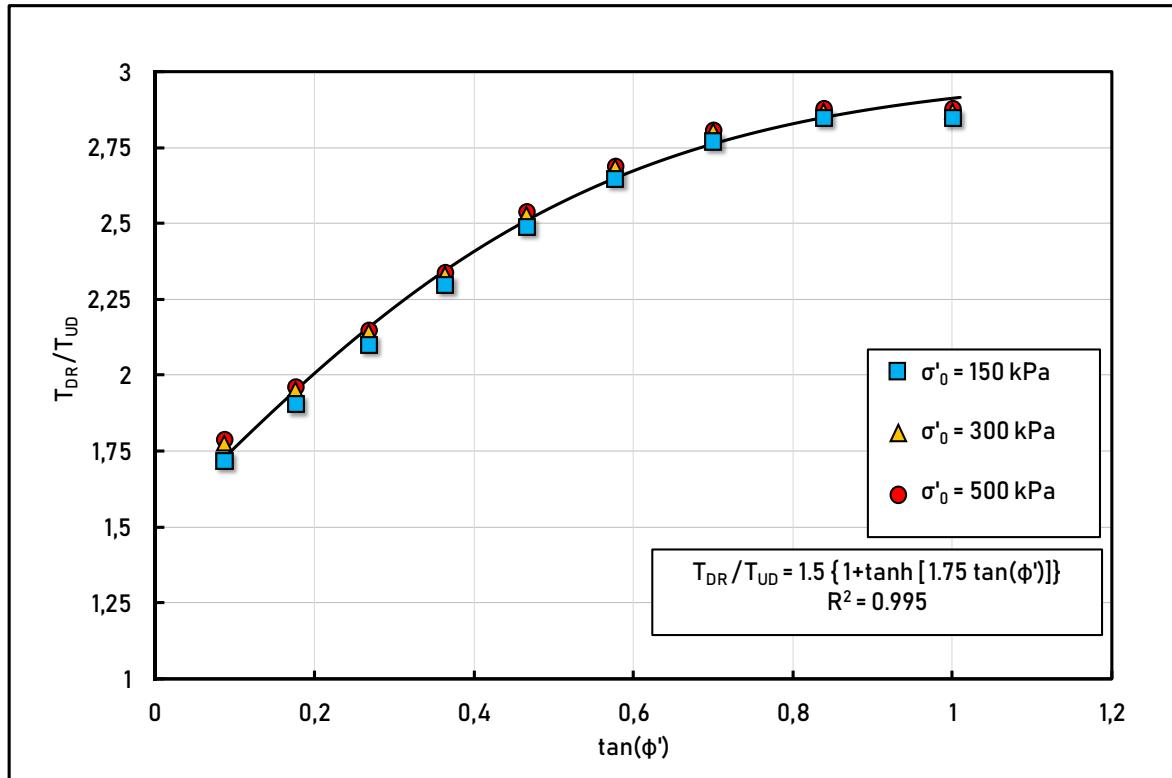

Figure 7. Drained to undrained torque ratio as function of internal friction angle (Forcelini et al., 2019).

The numerical predictions of $T_{0.1}/T_{UD}$ as well as corresponding fitted curves are plotted for different values of permeability coefficient in Figure 8 as function of $\tan\phi$. In this figure, symbols represent the numerical predictions, whereas continuous solid lines refer to fitted function defined by (9) and (10). The interest of the later expression lies in the fact they provide a simple correction of *in situ* measured torque when estimating undrained parameters.

In intermediate permeability soils in which vane test rotation lies between the drained and undrained conditions, the approach allows for correlating the torque measured at the standard rotation rate of $\omega_{SD} = 0.1 \, deg/s$ (partially drained) with a theoretically predicted undrained torque. Eq. 9 is a ready-to-use correlation for practitioners in routine engineering applications, but its application requires an independent assessment of soil permeability k to estimate $\bar{v}$.
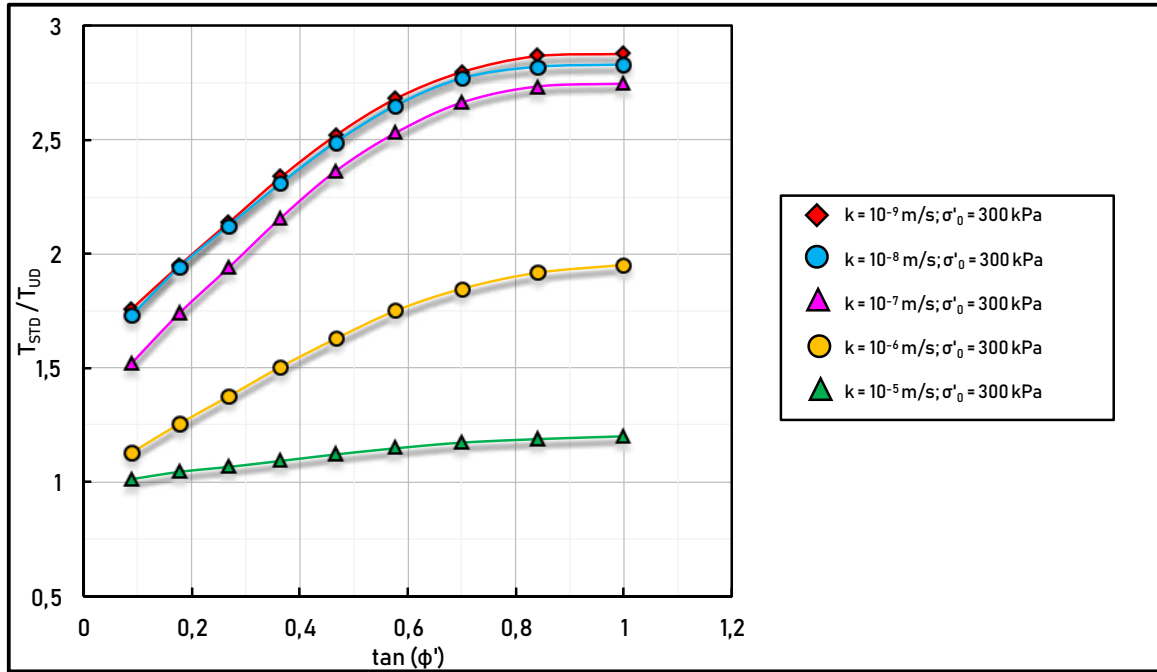

Figure 8. Ratio between mobilized torque at standard vane velocity and undrained torque as a function of soil friction angle (Forcelini at al., 2019).

4.3. Dilatometer (DMT)

There have been considerable recent updates on the interpretation of the flat dilatometer test (DMT) in transitional intermediate permeability soils that ultimately lead to developing alternative methods for predicting geotechnical parameters (Schnaid et al, 2018, 2020). In transitional soils, the after installation DMT readings are changing continuously with time due to excess pore pressures dissipation. By monitoring the variation in A-readings it is possible to measure a final drained A_D value or, alternatively, to extrapolate the results back to the origin to estimate an equivalent initial undrained A_{UD} value. The drained horizontal index $K_{D,dr}$ (drained) calculated from A_D can be used to estimate the internal friction angle (ϕ'), whereas the undrained horizontal index $K_{D,ud}$ (undrained) calculated from A_{UD} can be used to estimate the undrained shear strength. As for the CPT, if the penetration process is partially drained, the extrapolation to determine A_{UD} will be incorrect.

This integrated approach illustrated in Figure 9 offers a sound alternative to estimate both drained and undrained parameters from a single test. The approach can be introduced in practice with minimal costs by considering simple adaptations on procedures originally developed for clays.

The research that prompted these developments uses an instrumented flat dilatometer to measure pore pressures at the center of the blade during penetration (Schnaid et al, 2016) and the new Medusa DMT, which is an innovative device that is capable to autonomously perform dilatometer tests, providing higher quality continuous measurements of the membrane expansion (Marchetti et al, 2019).

Results using the Medusa DMT are shown in Figure 10, reporting data from silts in which the repeated DMT A reading is plotted against the elapsed testing time. As seen in this figure, readings show considerable variation with time because the pore pressure is continuously dissipating during approximately 150s. Finally, after completion of pore pressure dissipation, at the minimum lift-off pressure A_D, the membrane is inflated to measure the B pressure at 1.1mm displacement (Bf-reading).

Since both p_0 and p_1 are total stress measurements affected by the pore pressure regime taking place during penetration and membrane expansion., prediciton of soil properties from DMT measurements would require accounting for pore pressure dissipation after halting the blade. Only after full dissipation the ϕ'- K_D correlations for uncemented sands can be applied and, similarly, only under undrained conditions the S_u - K_D correlations established for clays can be considered. Prediction of properties from the DMT in tailings is presented later.
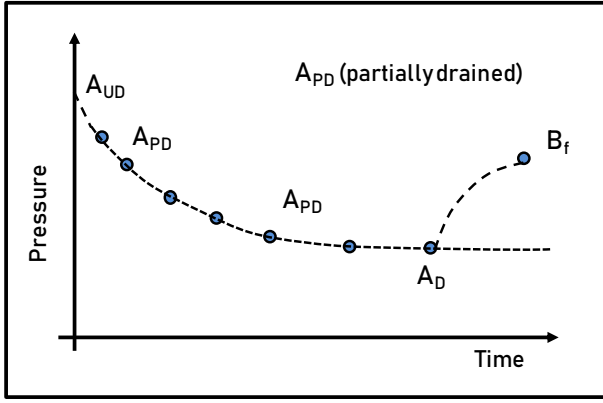
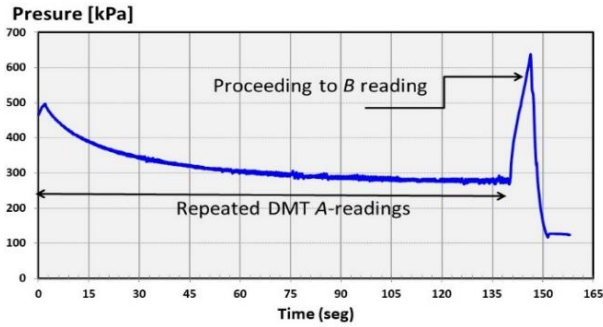**Figure 9.** Integrated approach for DMT in silts from A-decay test.

Figure 10. Typical Medusa DMT tests in silt (Odebrecht et al., 2020).

4.4. Standard Penetration Test (SPT)

Dynamic penetrometers are the simplest tests for site characterization. As a means of assessing liquefaction, tests such as the SPT fulfils the need to retrieve a disturbed soil sample to determine water content, fines content, and Atterberg Limits. Poor repeatability, lack of standardisation in test procedures, unknown values of energy delivered to the SPT rod and variable penetration rates during a single blow are limiting factors that may result in misleading predictions, particularly in transitional soils.

However, this test is still frequently used in tailings for evaluating soil properties and liquefaction potential. Correlations between blow count and liquefaction dating back to the mid 1960s have subsequently been revised by many researches in an attempt to produce a boundary line to differentiate between liquefiable and nonliquefiable conditions (Seed, 1979; Seed et al, 1985; Ishihara, 1993; Robertson and Wride, 1997). A threshold relation between the cyclic stress ratio and the N value of the SPT test was developed by Seed and Harder (1990) and has been used extensively worldwide.

The variable penetration rate on a single blow and the resulting complex pore pressure distribution around the sampler limits our ability to control the drainage conditions in dynamic penetration tests, and to develop rational interpretation methods for assessing soil parameters. In the design of tailings dams, however, there is one application for dynamic tests that merits consideration. It is still common to perform SPTs and CPTs in the same area, and to compare results to check for consistency and redundancy of information. Consequently, there is a need for reliable correlations

between the two tests, which is generally supported by empirical approaches linking the q_t/N_{60} ratios with mean grain size D_{50}, relative density or fines content (e.g. Robertson and Campanella, 1983; Suzuki et al, 1998; Idriss and Boulanger, 2004; Niven et al, 2005). This approach introduces errors when empirically converting N-value into equivalent q_t value because the dynamic penetration mechanisms contain several interdependent variables that cannot be condensed into a single blow count number. The use of N-value without further specifications should be discontinued and replaced by methods based on the principles of energy conservation and wave propagation analyses when calculating the dynamic penetration resistance.

Over the years, contributions have been presented to enhance the interpretation of dynamic tests and to relate the N-value and the CPT cone resistance (e.g. Schmertmann and Palacios, 1979; Skempton, 1986). In granular soils, for tests carried out under drained conditions, Odebrecht et al (2004) and Schnaid et al (2017) developed a rigorous solution that circumvent some of the inherent limitations associated to the SPT by calculating a dynamic penetration resistance (q_d):

$$q_d = \frac{F_d}{A_c} = \frac{\eta_3\eta_1(HM_hg)+\eta_3\eta_1(\Delta\rho M_hg)+\eta_3\eta_2(\Delta\rho M_rg)}{\Delta\rho\, A_c} \quad (11)$$

where F_d is the dynamic force, H the hammer height of fall, A_c the cross-section area of the penetrometer, M_h the hammer mass, M_r the rod mass, g the gravitational acceleration and η_1, η_2 and η_3 are efficiency factors. Equation 11 is valid for any penetrometer configuration but its applicability requires measuring force and acceleration signals for a proper calibration of coefficients, η_1, η_2 e η_3. No empirical or adjustments factors are needed when computing the dynamic penetration resistance q_d, which is calculated directly from the measured penetration values ($\Delta\rho$=N/30) recorded during dynamic tests.

The consistency between SPT and CPT records can then be made simply by comparisons between qd and qt which in principle should generate similar values by inherently accounting for density and stress level on a given material. An example illustrating the applicability of the proposed methodology is provided by results carried out along the crest of a starting dyke to elucidate the compaction conditions undertaken during construction. The water table depth was just below 20m. Figure 11 shows direct comparisons of three pairs of SPT and CPT data obtained from adjacent (5m spacing) soundings performed in fine sands placed as a compacted fill to retain slimes discharged at its upstream toe. The data reveal very similar penetration resistances computed from dynamic and static penetration tests. Overall, the dynamic SPT penetration resistance qd averages the cone penetration resistance qt with no systematic errors observed in these comparisons.

In conclusion, this general discussion on rate effects provides a broad picture of the major trends on *in situ* testing research carried out over the last decade in transitional soils. Recommendation for test procedures and for interpretation of testing data may lead to rational assessment of soil parameters.
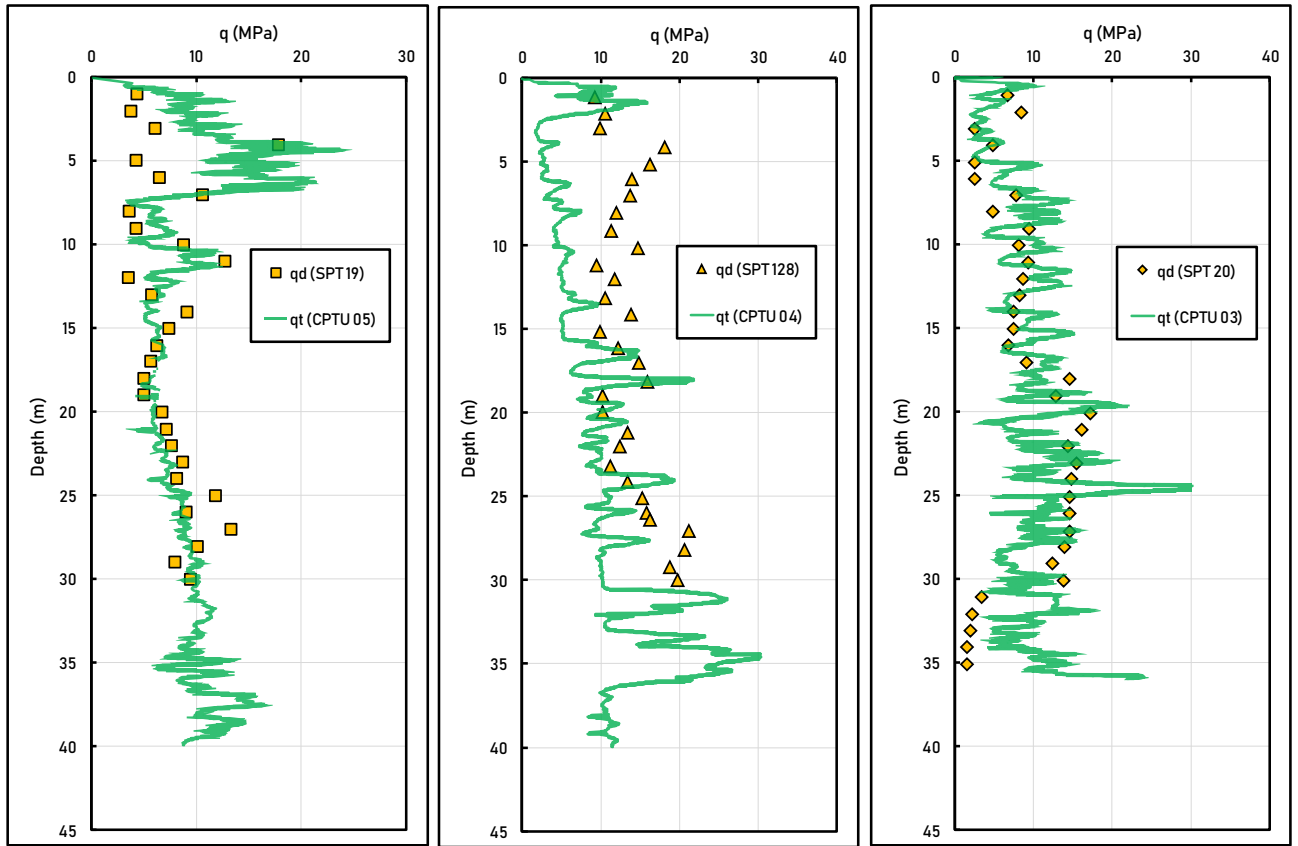
Figure 11. Comparisons between SPT and CPT in sandy-tailings forming a starting compacted dike.

5. Properties of tailings

As we advance in predicting the properties of tailings, it has become clear that the interpretation of *in situ* tests should be preceded by proper evaluation of the partial consolidation effects. In silts, the small strain shear modulus G_0 is not sensitive to loading rate, while the penetration resistance is rate dependent, the DMT procedure requires adaptations whereas the SPT penetration blow count remains empirical because the penetration event involves decreasing strain rate from impact until the device comes to rest.

In addition, it is advisable to use screening methods for assessing material behaviour type and potential liquefaction of tailings deposits previous to interpretation of *in situ* test results. Soil classification systems using the penetration tests are essentially based on at least two independent parameters, allowing initial assessment of geotechnical conditions by verifiable and reproducible procedures (see Robertson, 1990; 2010; 2016; Jefferies and Davies, 1998; Schneider, and Moss, 2011, Schnaid et al, 2020).

Bearing these conditions in mind, interpretation methods for assessment of the coefficient of consolidation, state parameter, friction angle and undrained shear strength are summarized herein. Field validation of the model predictions are discussed from a number of case studies reported in iron, gold and bauxite non-plastic tailings.

5.1. Coefficient of consolidation

Piezocone pore-water dissipation tests are routinely used to estimate the best global value of the *in situ*

coefficient of consolidation (c_h) from the variation in pore-water pressure with time. Interpretation rely either on one-dimensional cavity expansion and two-dimensional strain path method from which both monotonic and dilatory soil response can be modelled. The Teh and Houlsby method (1991) is considered the standard for monotonic pore pressure dissipation response and the Burns and Mayne method (1998) the alternative for dilatory response. For a given probe geometry and porous element location, the coefficient of consolidation c_h is expressed using a relationship that considers a time for 50% dissipation (t_{50}) from the CPTU tests:

$$c_h = \frac{t_{50}^* \, d^2 \, \sqrt{I_r}}{t_{50}} \tag{12}$$

where t_{50}^* a dimensionless time factor and I_r the rigidity index ($=G/S_u$). Albeit interpretation procedures are apparently simple to apply, there are uncertainties in assessing both the initial pore pressure u_i and the equilibrium *in situ* pore pressure u_0 in order to define t_{50}.

In intermediate permeability tailings the first limitation arises from the fact that interpretation of dissipation tests is complicated by partial consolidation effects occurring during penetration. The effect on dissipation tests following partial consolidation is shown to create errors in the interpretation of C_h because penetration is no longer fully undrained and the value of t_{50}^* estimated using undrained approaches under-predict the value actually measured after some consolidation. Based on the results of numerical analyses, an empirical approach was proposed by DeJong and Randolph (2012) to correct the estimated t_{50} (evaluated from the undrained

penetration assumption) by calculating an apparent time factor t_{50}^{ap} deduced from a family of curves conceived to account for different degrees of partial consolidation during penetration:

$$t_{50}^{ap}/t_{50}^{*} \approx 1 + \frac{1}{0.115 \, V_h^{1.2}} \qquad (13)$$

DeJong and Randolph (2012) recommended that when t_{50} is less than about 50s this solution helps predicting C_h values from tests carried out under the standard penetration rate of 20mm/s even when partial consolidation affects dissipation.

Secondly, it should be recognized that in tailing-retention dams the determination of phreatic surface location is influenced by pond location, anisotropic permeability of deposits, boundary flow conditions, permeable layers, among other factors (e.g. Vick, 1983). Since the error in estimating u_0 may impact the predicted t_{50}, two alternatives can be considered to overcome this limitation, the first being long dissipation tests up to at least 90% dissipation time to define the equilibrium pore pressure for accurate estimations of c_h. The second alternative was proposed by Mantaras et al. (2014) and consists on deriving an equation used to curve fitting the measured pore pressure dissipation data. A polynomial equation should be used to curve fitting the data, with the actual mathematical expression (degree) defined by the minimum r^2. First and second derivates correspond to the point of inflection of the normalized dissipation curve and define the theoretical value of t_{50}. This simple mathematical procedure captures the essence of physical models developed to interpret CPTU dissipation data, because in the methods developed by Teh and Housby (1991) and Burns and Mayne (1998) the dissipation curve exhibits an inflection point in which the curvature changes and produces a symmetrical shape in the U x T(log) curve. In practice a dissipation time of about 40%, to 50% should be enough to apply the proposed procedure, when the dissipation curve defines a well decay in pore pressures and allows for extrapolation of an approximately linear stretch of the dissipation curve in a semi log scale. Figure 12 illustrates the application of the method against the theoretical solution of Teh and Houlsby (1991). Since the equilibrium *in situ* pore pressure is no longer required to calculate the percentage of dissipation, one of the uncertainties in deriving C_h is eliminated.

The DMT offers an alternative procedure for estimating the horizontal coefficient of consolidation C_h by means of dissipation tests. The method consists in stopping the DMT blade at a given depth to monitor the decay of the total contact horizontal stress with time. Several slightly different procedures have been developed for this purpose (Robertson et al., 1988; Schmertmann, 1988; Marchetti and Totani, 1989). Marchetti and Totani (1989) suggested plotting the *A*-reading *versus log t* curve to identify the contraflexure point and the associated time (t_{flex}) in order to calculate the overconsolidated $C_{h,OC}$ (=$7cm^2/t_{flex}$) value. Correction factors are provided for estimating C_h in problems involving loading in the normally consolidated range.
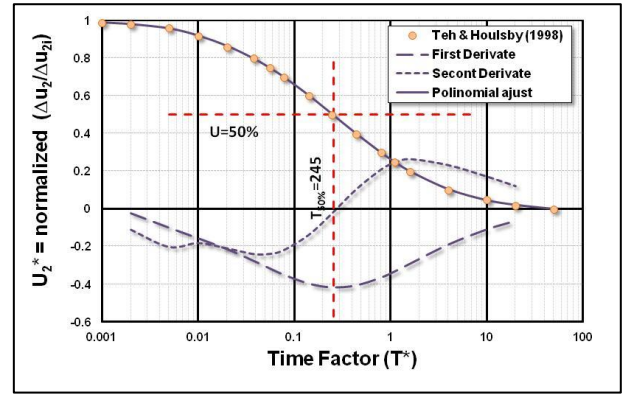

Figure 12. 1st and 2nd derivates of Teh and Houlsby (1991) theoretical solution for pore pressure dissipation (Mantaras et al., 2014).

5.2. State parameter

The behaviour of granular soils (i.e. all soils that are non-plastic) prior to the achievement of the critical state is largely controlled by the state parameter. A concept introduced by Wroth and Basset (1965) and developed by Been and Jefferies (1985), the state parameter ψ is defined as the difference between current void ratio e and critical state void ratio e_c, at the same mean stress. The state parameter represents the *in-situ* state of granular soils: negative values of ψ indicate dilative and strain-hardening response in undrained shear, whereas positive ψ contractive and strain-softening behaviour. Jefferies and Been (2016) and Shuttle and Cunning (2007) suggested that when a soil has a state parameter ψ greater than -0.05, strain softening and strength loss in undrained shear are to be expected and thus the soil is prone to liquefaction. This recommendation was introduced for clean sands, but has been gradually extended to a much wider range of soils and for non-plastic tailings.

Because of the difficulty in sampling in granular soils, assessment of ψ values depend primarily on penetration tests. Current engineering practice relies heavily on correlations established for CPTU measurements, although other alternatives such as the seismic-cone and cone-pressuremeter can enhance interpretation. However, most available methods embrace the concept of a linear critical state line, developed from cavity expansion theory used to model drained penetration without due consideration for strain softening, and calibrated against laboratory and calibration chamber test results in clean uniform sands. Since the shape of the CSL in the $e - p_0$ space controls the value of the state parameter, it is reasonable to expect that although CPTU methods provide screening for liquefaction susceptibility, they should be viewed as the first step towards a judicious choice of further investigation from laboratory tests.

A summary of available methods for determining the state parameter *in situ* is presented in Table 1, including the auxiliary dimensionless equations inherent to each analytical method.

A method to estimate ψ using normalized CPTU results based on effective stress cavity expansion simulations is reported by Plewes et al. (1992) and Jefferies and Been (2006). The method (Eq. 14 in Table

1) inherently accounts for soil compressibility and can provide a direct estimative of ψ from the measured q_t, pore pressure parameter B_q, mean effective stress p' and friction ratio F_r (which is empirically related to the slope of the critical state line λ). Robertson (2010) suggests a simplified and approximate CPTU relationship from which the state parameter is estimated from q_t, F_r and σ'_{v0} (Eq. 15).

Since interpretation of *in situ* tests in granular soils is complex, a single recommendation is to use correlations with mechanical properties based on the combination of measurements from independent tests such as the ratio of the elastic stiffness to cone resistance (G_0/q_t) and the ratio of cone resistance to pressuremeter limit pressure (q_t/P_l). From the seismic cone test in granular soils, Schnaid and Yu (2005) developed a simple theoretical approach to estimate ψ using the ratio of elastic stiffness, as estimated from the measured shear wave velocity, to the cone resistance. In Eq (16) in Table 1 the critical state soil model proposed by Collins et al (1992), associated to the effective cone resistance estimated from spherical cavity limit pressure in Ladanyi and Johnston (1974), was combined to the elastic stiffness, soil void ratio and stress level correlation proposed by Lo Presti *et al.* (1997).

The Collins *et al* (1992) solution was also the basis for the interpretation of the sate parameter from cone-pressuremeter tests. In the theoretical development, the 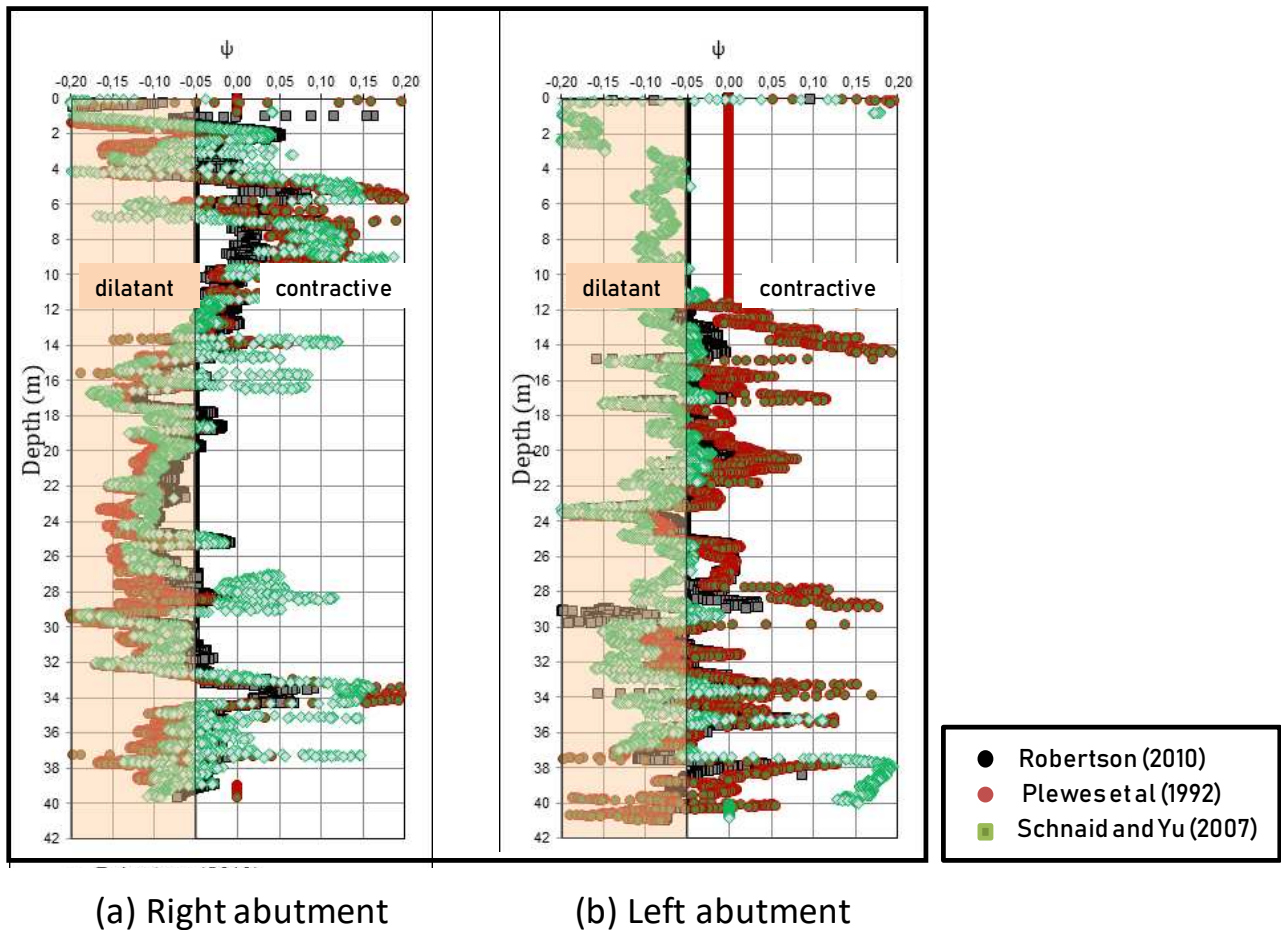authors have assumed that both the cone resistance q_t and the pressuremeter limit pressure P_L are strongly related to the limit pressure of spherical (P'_{ls}) and cylindrical (P'_{lc}) cavities respectively (Eq. 17 in Table 1).

An example illustrating the state parameter variation with depth from SCPTU tests carried out in the beach close to the upstream face of a tailings dam, towards the right and left abutments respectively, is shown in Figure 13. The two CPT-based methods (Plewes et al, 1992; Robertson, 2010) yielded fairly similar trends and identified zones of compressible tailings susceptible to liquefaction. By adding the contribution from soil stiffness, the SCPT-based state parameter variation (Schnaid and Yu, 2007) agreed sufficiently well with the CPT values in the right abutment, but indicated a predominance of dilative tailings clustered along ψ=-0,05 in the left abutment, in contrast with positive ψ values estimated from the cone. Liquefiable layers were detected close to the surface and at greater depth.

It is important to draw attention to the fact that none of these methods give a correct estimate of ψ in non-plastic silt tailings. The Plewes et al (1992) and Jefferies and Been (2016) methods can be applied over a wide range of soils (sands through to silts), as long as you have an accurate estimate of compressibility. Likewise, Robertson (2010) can be used over a wide range of soils, but one should rely on empirical procedures supported by classification charts. Schnaid & Yu (2005) method was calibrated against laboratory tests on clean sands that have little or no microstructure.

Table 1. State parameter calculation.

Method/test	Equation	Auxiliary equations	
Piezocone + laboratory tests (Plewes et al, 1992; Jefferies and Been, 2016)	$\Psi = \dfrac{-ln\left(\dfrac{\overline{Qp}}{k}\right)}{\overline{m}}$ Equation (14)	$\overline{Qp} = \dfrac{(q_t - \sigma_0)}{\sigma'_0}(1 - B_q)$ $\bar{k} = \left(3 + \dfrac{0,85}{\lambda}\right)M$	$\overline{m} = 11,9 + 13,3\lambda$ $\lambda = \dfrac{Fr(\%)}{10}$
Piezocone (Robertson, 2010)	$\Psi = 0.56 - 0.33 logQ_{tn,cs}$ Equation (15)	$Q_{tn} = [(q_t - \sigma_{v0})/p_a](p_a/\sigma'_{v0})^n$ $n = 0.381(I_c) + 0.05\left(\sigma'_{v0}/p_a\right) - 0.15 \leq 1,0$ $Q_{tn,cs} = K_c Q_{tn}$ $K_c = 1.0 \ if \ I_c \leq 1.64$ $K_c = 5.581I_c^3 - 0.403I_c^4 - 21.63I_c^2 + 33.75I_c - 17.88 \ \ if \ I_c > 1.64$	
Seismic cone (Schnaid & Yu, 2007)	$\psi = -0.52\left(\dfrac{p'}{p_a}\right)^{-0.07} + 0.18 \, ln\left(\dfrac{G_o}{q_t}\right)$ Equation (16)	$q_t = q_{tD}$ (drained)	
Cone-pressuremeter (Yu, Schnaid & Collins, 1996)	$\psi = 0.4575 - 0.2966 \, ln\dfrac{q_t}{P_L}$ Equation (17)	$q_t = q_{tD}$ (drained)	
Dilatometer Yu (2004) Robertson (2012)	$\psi = -0.002\left(\dfrac{K_D}{K_0}\right)^2 + 0.015\left(\dfrac{K_D}{K_0}\right) + 0.0026$ Equation (18)	K_D drained	
	$\psi = 0.56 - 0.33 log(25K_D)$ Equation (19)	K_D drained	

Figure 13. State parameter predictions from piezocone and seismic-cone tests (silt, iron ore tailings).

(a) Right abutment   (b) Left abutment

5.3. Angle of friction

Slope stability analysis is a minimum requirement to be performed for all tailings storage facilities to verify that all safety factors associated with the governing load cases of all possible modes of slope failure meet or exceed the minimum requirements of standards. Numerical simulations or simple limit equilibrium analyses can be used to calculate slope stability that, under drained conditions, is performed using the Mohr-Coulomb yield criterion with ϕ' indicating the mobilized effective stress angle of internal friction. Described as the peak friction angle ϕ'_p, it is the combination of the angle of friction at critical state ϕ'_{cs} (highly dependent on particle shape, size and roundness) and the dilation component produced by the particle arrangement. The variation of peak friction angle and dilation rate as a function of confining pressure and density is well-established since 1960s (e.g. Rowe 1963, Bolton, 1986, Jamiolkowski et al., 1985; Santamarina and Cho, 2004; Cho et al., 2006).

From an extensive laboratory database on sands, Been and Jefferies (1985) equated the triaxial peak friction angle as a function of the state parameter for sands with fines contents ranging from 0 to 18% (see Eq 20 in Table 2). Later an expanded database including 240 drained triaxial tests indicated a simple linear trend between Ψ and ϕ' (Eq 21 in Table 2) with a fairly narrow bandwidth for the tested data (Jefferies and Been, 2016).

Because of the difficulty in sampling granular tailings, properties measured in the laboratory are linked to the in situ soil state by field tests. In practice, interpretation of soil state depends primarily on penetration tests. Estimating the peak friction angle ϕ'_p from the CPT is supported by analytical methods, numerical simulations and empirical correlations, as reported by de Mello et al (1971), Jamiolkowski et al. (2001), Yu and Mitchell (1998) and Mayne (2009), this last reference reported as the 2nd J. Mitchell Lecture. Methods established from spherical cavity expansion theory and limit plasticity formulation, validated against reference calibration chamber tests, are summarized in Table 2 and expressed in terms of the normalized cone tip resistance Q (= q_t/σ'_{vo} or q_t -σ_{vo} /σ'_{vo}).

Some correlations rely on cone penetration resistance only, whereas the problem of expanding a spherical cavity depends heavily on soil stiffness, i.e. without soil stiffness it is impossible to accurate predict ϕ from q_t. Methodologies for using the CPT for determining ψ highlighted this dependency by demonstrating that G_0/q_t can assist screening for liquefaction potential. Seeking to capture the scatter inherently observed in CPT correlations, the state parameter Eq. (16) is combined with the CPT expression proposed by Kulhawy & Mayne (1990) (Eq. 23):

$$\phi'_p = 17{,}6° + 11{,}0\log[(G_0/\sigma'_{v0})/(\sigma_{atm}/\sigma'_{v0})^{0,5}] - 13{,}8\left(\frac{p'}{p_a}\right)^{-0{,}07} - 25.54\,\psi \qquad (20)$$

Table 2. Effective friction angle calculation from drained test results.

Test	Correlation	Reference
Laboratory	$\phi'_{p,tc} - \phi_{cs} = A[exp(-\psi) - 1]$ *A from 0.6 to 0.95* Equation (21)	Been & Jefferies (1985) *
	$\phi'_p = \phi_{cs} * (1 - 5/3\psi)$ Equation (22)	Jefferies & Been (2016)*
Piezocone	$\phi'_p = \text{arctg}[0,1069 + 0,3918 \log(q_t/\sigma'_{v0})]$ Equation (23)	Robertson & Campanella (1983)
	$\phi'_p = 17,6° + 11,0 \log[(q_t/\sigma_{atm})/(\sigma'_{v0}/\sigma_{atm})^{0,5}]$ Equation (24)	Kulhawy & Mayne (1990)
	$\phi'_p = \arctan[0,1 + 0,38 \log(q_t/\sigma'_{v0})]$ Equation (25)	Lunne et al. (1997)
	$\phi'_p = \phi'_{cs} + 15.84 \left(\log Q_{tn,cs}\right) - 26.88$ $Q_{tn} = [(q_t - \sigma_{v0})/p_a](p_a/\sigma'_{v0})^n$ $Q_{tn,cs} = K_c Q_{tn} \quad K_c = f(I_c)$ Equation (26)	Robertson (2012)
Sesmic-cone	$\phi'_p = \arctan[0,38 \log(G_0/\sigma'_{v0}) - 0,92\,\psi - 0,28]$ Equation (27)	ψ from eq (13 from Table 1)
Cone-pressure-meter	$\phi'_{ps} = \dfrac{14.7}{ln\,I_s}\dfrac{q_c}{\psi_L} + 22.7$ Equation (28)	Yu & Houlsby (1991) #
Dilatometer	$\phi' = \phi_{cs} + \alpha \cdot \log(K_D); \alpha \approx 14$ Equation (29)	Schnaid et al (2020)*
SPT	$\phi'_p = \left[\dfrac{(N_{60})}{12.2 + (\sigma'_{vo}/\sigma_{atm})}\right]^{0.34}$ Equation (30)	Schmertmann (1975)+
	$\phi'_p = 20° + \sqrt{15.4(N_1)_{60}}$ Equation (31)	Hatanaka & Uchida (1996)+
* Triaxial friction angle (in degrees) *# Plane strain friction angle (in degrees)* *+ N-values corrected for energy and/or stresses*		

Similarly, Eq (16) can be combined to the CPT expression proposed by Lunne et al., (1997) (Eq. 24):

$$\phi'_p = \arctan\Big[0,10 + 0,38\log(G_0/\sigma'_{v0}) - 0,48\left(\frac{p'}{p_a}\right)^{-0,07} - 0,92\,\psi\Big] \qquad (32)$$

By considering $K_0=1$ and assuming a reference mean stress of 100kPa, Eq (32) simplifies as:

$$\phi'_p = \arctan[0,38\log(G_0/\sigma'_{v0}) - 0,92\,\psi - 0,28]$$
(Equation (27)bis, Table 2)

Eq (26) indicates the need to account for soil stiffness when determining ϕ'_p from ψ values estimated from CPT data, which in fact requires seismic cone data. We can now refer to Figure 14 established by Been and Jefferies (2016), where the triaxial compression friction angle is expressed as a function of the state parameter as:

$$\left(\phi_{p,tc} - \phi_{cs}\right) = 1 - \frac{5}{3}\psi \quad \text{(Equation (22) bis – Table 2)}$$

and compare the laboratory data to CPT predictions of ϕ'_p from eq (26) for G_0/σ'_{v0} ratios ranging from 150 to 400. Eq. (26) appears to capture the experimental variation between ϕ'_p and ψ, including the scatter of results that is imposed by material compressibility on CPT penetration resistance. As most of the proposed equations presented herein, they apply to soils with little or no microstructure.
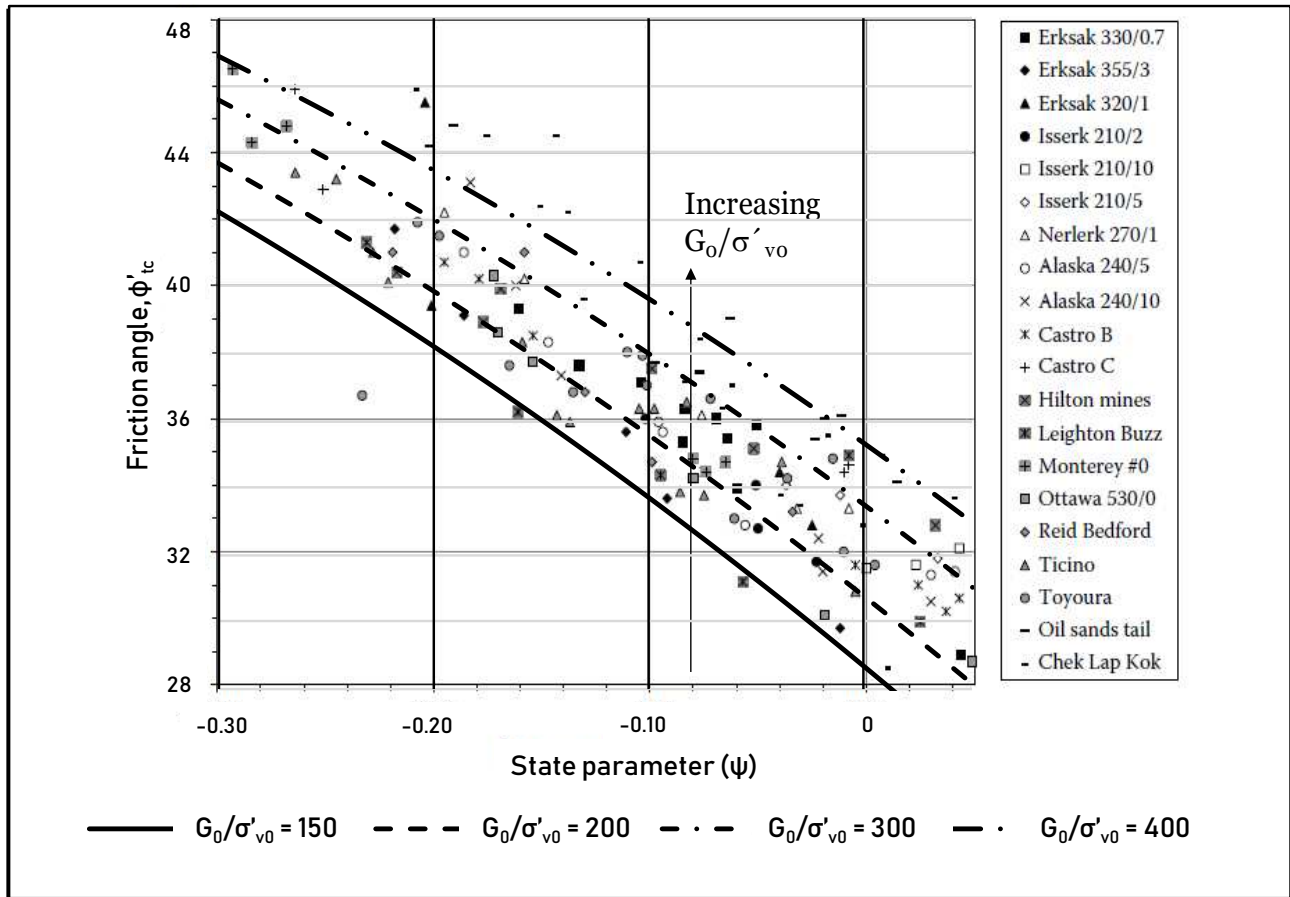
Figure 14. Peak friction angle in standard drained compression from the state parameter, (Been & Jefferies, 2016) with predictive method using the seismic cone.

Other correlations available to estimate ϕ' directly from in situ testing measurements are listed in Table 2. SPT interpretation for evaluating ϕ' is mainly empirical (e.g. Stroud, 1988; Kulhawy and Mayne, 1990; Schmertmann, 1975; Skempton, 1986).

Alternative methods listed in Table 2 include the dilatometer (Marchetti, 1980; Odebrecht et al, 2020), the pressuremeter and the cone-pressuremeter (e.g. Yu & Houlsby, 1991; Schnaid and Houlsby, 1992; Yu, 2000). Prediction of the friction angle in granular soils using the DMT is primarily based on KD which is just a normalisation of po with respect to the vertical effective stress. From the proportionality between KD and penetration resistance, and then to tip cone resistance, Schmertmann (1982) proposed a method to estimate ϕ' using the bearing capacity theory of Durgunoglu & Mitchell (1975). This approach was later adapted by Marchetti (1985) in a graphical representation that enables to estimate ϕ' from k_0 and q_t or K_D. For tailings, the original ϕ' - K_D correlation for uncemented sands established by Marchetti has been modified, and a new correlation is proposed in which ϕ' is expressed as a function of K_D and the critical state friction angle ϕ_{cs}:

$$\phi' = \phi_{cs} + \alpha \cdot \log(K_D) \quad \text{(Equation (28)bis – Table 2)}$$

An evaluation of α of Eq. (27) to estimate ϕ' was made by comparisons with values estimated from piezocone tests, yielding a value of $\alpha=14$ (Schnaid et al, 2020). Robertson (2012) suggested that $Q_{tn,cs}=25K_D$ for

uncemented sands that, when combined to the equation for ϕ' based on $Q_{tn,cs}$, yield a similar relationship with a slightly higher value for α.

Some of the proposed correlations listed in Table 2 require the determination of the critical state friction angle. As guidance for design, Figure 15 shows a relationship between the critical state angle of shearing resistance ϕ_{cs} and mean particle size D_{50} for different non-plastic silty tailings (modified from Li et al, 2018). It can be seen that most ϕ_{cs} values for different silt tailings fall within the narrow range at about $33° \pm 2°$, despite the marked variability in mineralogy and particle shape expected for these materials. For sands (gray symbols in Figure 15), the increase in particle irregularity causes a significant increase in the critical state friction angle ϕ_{cs} (e.g. Cubrinovski and Ishihara, 2002; Cho et al, 2006), which is not observed in tailings. It appears that crushing and grinding produce particles with low angularity or, in cases where minerals are angular, particle breakage occurs at relatively small shear strains even at low confining stresses (see Bedin et al., 2012).

5.4. Undrained shear strength

The undrained shear strength of tailings, common in all soils, depends on the mode of failure, rate of shearing, soil anisotropy and stress history (e.g. Ladd et al, 1977; Jamiolkowski et al, 1985). Short term undrained shear strength is therefore not a unique soil parameter, being strongly dependent upon the method by which it is

determined. Since liquefaction in loose tailings largely controls the factor of safety, there is substantial interest in estimating the peak and residual strengths $S_{u,p}$ and $S_{u,res}$ from both laboratory and *in situ* tests. The brittle strength reduction from peak to residual is the cause of collapse of dams by both static and cyclic liquefaction.
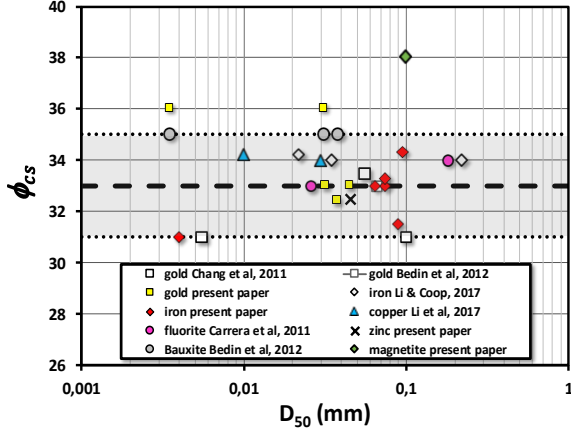
Figure 15. Critical state friction angle in tailings (modified from Li et al., 2018)

In discussing the shear strength of liquefied soils, it is necessary to distinguish among the different measures of strength that can be used to characterize the *in situ* stress-strain response of saturated strain softening soils:

- The ultimate shear resistance, or critical-state strength, which can be measured in an undrained monotonic laboratory element test, is denoted as $S_{u,cs}$;
- The residual shear resistance that corresponds to the available post-peak strength determined from an undrained monotonic or cyclic laboratory element test is denoted as $S_{u,r}$; and
- Liquefied shear strength, denoted as $S_{u,liq}$, refers to the shear resistance that a liquefied soil mobilizes in the field, that is not replicated in laboratory element tests.

Although considerable research and development have gone into interpreting *in situ* test data to enhance our ability in predicting undrained strength, this issue is far from being resolved and is the main source of uncertainty in tailings dam stability design.

5.5. Peak undrained shear strength

Predicting peak undrained shear strength follows critical state soil mechanics theory. For materials that conforms with CSSM, normalization in triaxial compression strength for normally consolidated specimens is obtained from (Wroth, 1984):

$$\left(\frac{S_{u,tc}}{p_o'}\right)_{nc} \approx \frac{M}{2}\left(\frac{1}{2}\right)^{0,8} \tag{33}$$

where M is the critical stress ratio and p_o' is the mean effective stress. Similarly, Wroth (1984) demonstrated that for isotropically normally consolidated conditions,

the undrained strength ratio obtained from tests in plane strain would be:

$$\left(\frac{S_{u,ps}}{\sigma_{vo}'}\right)_{nc} = sin\phi_{ps}\left(\frac{1}{2}\right)^{\Lambda} \approx \frac{1}{2}sin\phi_{ps} \tag{34}$$

These equations give reference values for design that assist on the interpretation of *in situ* testing data. A summary of available formulations to calculate the peak undrained shear strength is shown in Table 3.

Since the CPTU cannot directly measure the undrained shear strength, assessment of S_u relies on a combination of theory and empirical correlations. As extensively discussed throughout this paper, interpretation of results is only possible when penetration is fully undrained, and guidance was provided from the normalized velocity approach (V).

For undrained CPTUs, the penetration resistance q_t can be related to the peak undrained shear strength $S_{u,p}$ by the theoretical penetration factor N_c and the *in situ* total stress σ_0 (either vertical or mean total stress). The theoretical solutions available for determining N_c can be attained by bearing capacity theory, cavity expansion theory, strain path method and finite element method (e.g. Yu & Mitchell, 1998; Yu, 2004). For tailings, the correlation between penetration resistance and undrained shear strength is site specific, depending on the unit weight and the N_c factor of the tailings. The CPTU correlation between $S_{u,p}$ and q_t is expressed as:

$$S_u = \frac{q_t - \sigma_{vo}}{N_{kt}} \qquad \text{(Equation (35)bis – Table 3)}$$

where N_{kt} is an empirical cone factor and σ_{v0} is the total *in situ* vertical stress. Values of N_{kt} range from 10 to 20 and are influenced by soil plasticity. In the absence of vane test for a reference undrained strength, the correlation proposed by Lunne et al (1997) offers a sounding first approximation ($N_{kt} = 22 - 13,33\ B_q$).

S_u can also be expressed directly as a function of excess pore water pressure as (e.g. Battaglio et al, 1981):

$$S_u = \frac{(u_2 - u_o)}{N_{\Delta u}} \qquad \text{(Equation (36)bis – Table 3)}$$

where NΔu can be approximated using $N_{\Delta u} = 4 + 6Bq$. A straightforward procedure is to estimate $S_{u,p}$ from both penetration resistance and excess pore water pressure, checking the consistency between the two approaches. Figure 16 shows a CPTU test in fine-grained iron tailings, in which cone penetration (q_t), pore pressure (u_2), pore pressure ratio (B_q) and undrained peak strength are plotted against depth. In the soft layer below 28m the excellent comparisons of S_u values derived from N_{kt} and from $N_{\Delta u}$ indicate fully undrained penetration, otherwise S_u derived from u_2 would be significantly smaller than those estimated from q_t, as observed in the superficial layer.

Table 3. Peak undrained shear strength

Test	Correlation	Auxiliary equations#	References
Piezocone	$S_u = \dfrac{q_t - \sigma_{vo}}{N_{kt}}$ Equation (35)	$N_{kt} = 22 - 13,33\, B_q$ and $N_{kt} \geq 9$	Lunne et al, (1997)
Piezocone	$S_u = \dfrac{(u_2 - u_o)}{N_{\Delta u}}$ Equation (36)	$N_{\Delta u} = 4 + 6Bq$	Battaglio et al, (1981)
T-bar or ball penetrometer	$S_u = \dfrac{q_{net}}{N_{T-bar}}$ or $S_u = \dfrac{q_{net}}{N_{ball}}$ Equation (37)	$N_{T-bar}(ave) = 10,5$ $N_{ball}(ave) = 10,5$	Randolph and Andersen (2006)
Vane test	$S_u = \dfrac{6T_m}{7\pi D^3}$ Equation (38)		Chandler (1988)
Dilatometer	$S_u = 0.22\sigma'_{vo}(0.5K_D)^{1.25}$ Equation (39)	$KD = KD,ud$	Marchetti (1980)
# Reference values for soft clays in triaxial compression or direct shear			

Full flow probes, including T-bar and ball penetrometers (Randolph, 2004) developed for soft clay are alternatives for fine granular tailings. Penetrometer resistances measured during penetration should be corrected for the unequal pore pressure and overburden pressure effects using the following simplified equation (Randolph and Andersen 2006; Randolph et al, 2007):

$$q_{T-bar} \text{ or } q_{ball} = q_m - [\sigma_{vo} - u_0(1-\alpha)]\,A_s\big/A_p$$
Equation (37)bis – Table 3)

where q_{T-bar} and q_{ball} are the net penetration resistances for T-bar and ball penetrometer, respectively, qm is the measured resistance, u0 is the hydrostatic water pressure, α is the net area ratio (ranging from 0.6 to 1.0), As is the cross-sectional area of the connecting shaft and Ap is the projected area of the penetrometer in a plane normal to the shaft. Full-flow penetrometers proved to be useful in uniform soft clays that show little strain softening for peak undrained strength, but the cone factor shows large variations in sensitive soils. There is relatively little experience in contractive strain softening silts where research is still required to establish appropriate testing procedures.

The field vane test (FVT) measures undrained shear strength (S_u) directly in undrained materials. Cone penetration and pore pressure dissipation testing carried out prior to FVT are necessary to define stratigraphy and determine zones of fine-grained tailings in which FVT may be appropriate. Undrained conditions are assured when v/k is greater than 10+5 and under these conditions are achieved, high-quality FVT can be used to calibrate the bearing factors (Nkt) for CPT and full penetrometers and to determine shear strength of tailings. Otherwise, corrections to the measured torque should be applied using Eq. (9).

For the flat dilatometer test (DMT), a testing procedure and interpretation method were proposed for the characterization of silts (Schnaid et al, 2016). The method aimed at compensating for errors that are introduced by the partial-drainage conditions that take place around the DMT blade (errors induced by dissipation during penetration of the blade should be evaluated independently). The method consists in monitoring the variation in A-readings until the completion of dissipation, when the pressure-time curve has flattened around a minimum pressure (see Figure 9 presented previously). A full A-decay curve is then available for interpretation and, in this case, a mathematical function can be selected to best fit the series of data points. The Weibull distribution (Weibull, 1951) can be adopted as a reference to represent the S-shape curve in an A–log(t) diagram.

The calculated $A_{0,UD}$ reading (for t =0) is used as input value to determine the p0 pressure using the following formulae:

$$p_{0,UD} = 1,05\big(A_{0,UD} - Z_m + \Delta A_{cal}\big) \tag{40}$$

where ΔA_{cal}, is obtained from membrane calibration and Zm is the gage zero offset (note that the term ΔB_{cal} proposed by Marchetti (1980) has been omitted from Eq$p_{0,UD} = 1,05\big(A_{0,UD} - Z_m + \Delta A_{cal}\big)$ (42). Since in the Medusa DMT Z_m is zero (single calibration gage) and the 1.05 factor used in combination with the (B – Delta B) is eliminated, Eq. $p_{0,UD} = 1,05\big(A_{0,UD} - Z_m + \Delta A_{cal}\big)$ (42) can be expressed simply as:

$$p_{0,UD} = A_{0,UD} + \Delta A_{cal} \tag{41}$$

The horizontal-stress index K_D is then expressed as a function of p_0 (Eq. $p_{0,UD} = A0,UD + \Delta A𝑐al𝑎$ (43)), allowing S_u to be estimated from the correlation proposed by Marchetti (1980):

$$S_u = 0.22\sigma'_{vo}(0.5K_D)^{1.25} \text{ (Equation (39)bis – Table 3)}$$

Preliminary results demonstrate that the method is effective and can be introduced in practice with marginal

increase in costs by considering simple adaptations to procedures originally developed for clays.
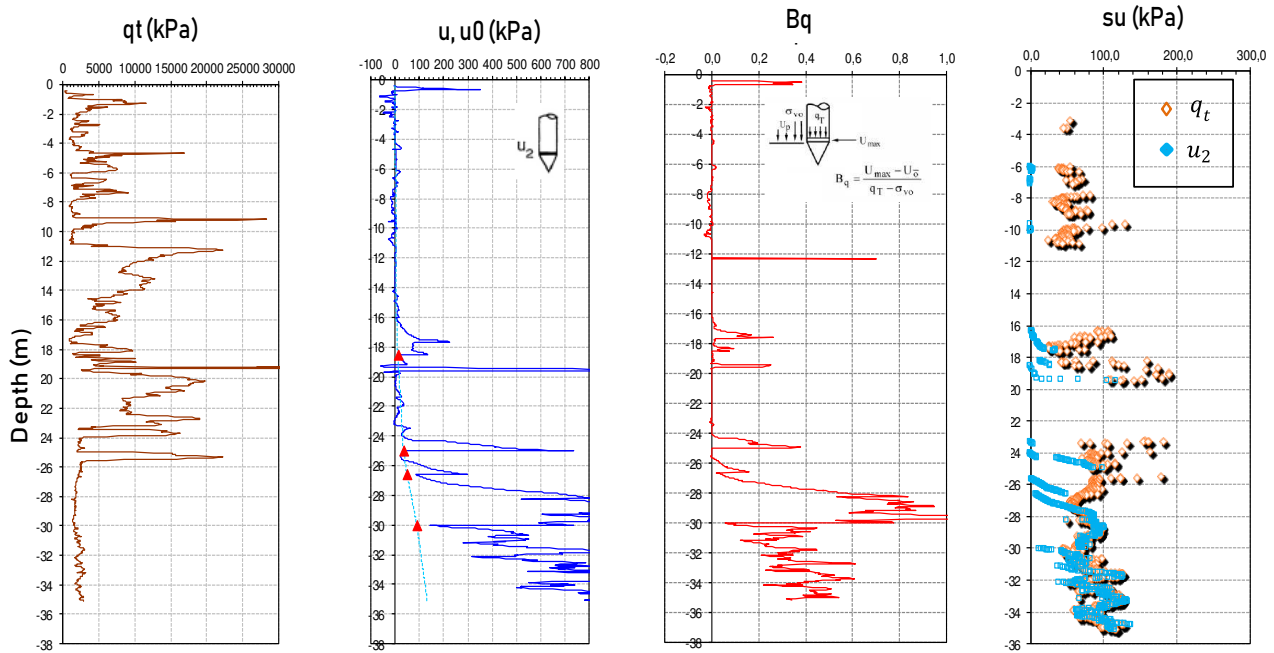

Figure 16. CPTU test results in iron tailings.

For the flat dilatometer test (DMT), a testing procedure and interpretation method were proposed for the characterization of silts (Schnaid et al, 2016). The method aimed at compensating for errors that are introduced by the partial-drainage conditions that take place around the DMT blade (errors induced by dissipation during penetration of the blade should be evaluated independently). The method consists in monitoring the variation in A-readings until the completion of dissipation, when the pressure-time curve has flattened around a minimum pressure (see Figure 9 presented previously). A full A-decay curve is then available for interpretation and, in this case, a mathematical function can be selected to best fit the series of data points. The Weibull distribution (Weibull, 1951) can be adopted as a reference to represent the S-shape curve in an A–log(t) diagram.

The calculated $A_{0,UD}$ reading (for t =0) is used as input value to determine the p_0 pressure using the following formulae:

$$p_{0,UD} = 1,05\left(A_{0,UD} - Z_m + \Delta A_{cal}\right) \tag{42}$$

where ΔA_{cal}, is obtained from membrane calibration and Zm is the gage zero offset (note that the term ΔB_{cal} proposed by Marchetti (1980) has been omitted from Eq $p_{0,UD} = 1,05\left(A_{0,UD} - Z_m + \Delta A_{cal}\right)$ (42). Since in the Medusa DMT Z_m is zero (single calibration gage) and the 1.05 factor used in combination with the (B – Delta B) is eliminated, Eq. $p_{0,UD} = 1,05\left(A_{0,UD} - Z_m + \Delta A_{cal}\right)$ (42) can be expressed simply as:

$$p_{0,UD} = A_{0,UD} + \Delta A_{cal} \tag{43}$$

The horizontal-stress index K_D is then expressed as a function of p_0 (Eq. $p_{0,UD} = A0,UD+\Delta A⬚cal⬚$ (43)), allowing S_u to be estimated from the correlation proposed by Marchetti (1980):

$$S_u = 0.22\sigma'_{vo}(0.5K_D)^{1.25} \text{ (Equation (39)bis – Table 3)}$$

Preliminary results demonstrate that the method is effective and can be introduced in practice with marginal increase in costs by considering simple adaptations to procedures originally developed for clays.

5.6. Residual undrained shear strength

This section introduces the methods currently adopted for estimating the undrained residual (post-liquefaction) shear strength ($S_{u,r}$). The undrained residual strength has also been referred to as the undrained steady-state shear strength (Poulos, 1981), the undrained critical shear strength (Seed, 1987) or the liquefied shear strength (Olson & Stark, 2002).

The post-seismic stability of embankments should be assessed from reduced shear strength to account for increased pore pressures due to cyclic stresses. New guidelines require strength reduction to be applied to all materials independently whether the factor of safety against liquefaction (FS_liq) is greater or less than 1.0.

Following critical state soil mechanics, the undrained residual strength ratio can be obtained from (e.g. Jefferies and Been, 2016):

$$\frac{S_{u,r}}{p_o'} = \frac{M}{2} exp\left(\frac{\psi}{\lambda}\right) \qquad (44)$$

where λ is the slope of the critical state line in the $e_0 - lnp'$ plot and p_o' the mean effective stress. Simple interpretation of critical state parameters from reconstituted samples give reference values of $S_{u,r}/\sigma_{v0}'$ for stability analysis, recalling that the ratio of λ/ψ typically ranges from -2.0 to +2.0 yielding $S_{u,r}/\sigma_{v0}'$ ratios from 0.04 to 0.12.

Departing from this concept, Jefferies and Been (2016) demonstrated that the residual stress ratio $S_{u,r}/\sigma_{v0}'$ can be calculated from the normalized cone resistance $Q = [(q_t - \sigma_{v0})/\sigma_{v0}']$ assuming that K_0 is close to unity (Jefferies and Been, 2016):

$$\frac{S_{ur}}{\sigma_{vo}'} = \frac{M}{2}\left(\frac{Q}{k}\right)^{1/m\lambda} \qquad (45)$$

In doing so, it is necessary to assess the critical state coefficients M, λ, k and m independently from laboratory tests, recalling that representativeness of lab data to field conditions is always an issue.

An alternative for estimating the residual shear strength may be the full-flow penetrometers. Recommended procedures and interpretation methods for tests in clays can be adapted for intermediate gran size tailings, especially in the evaluation of so called remolded strength (and soil sensitivity) which is accomplished after several large amplitude displacement cycles (e.g. Randolph and Andersen 2006; Zhou and Randolph 2009). Specific protocols are required to define optimized frequency and amplitude of cycles to estimate the undrained residual stress in tailings. This is currently a subject of research in silty tailings where the rate of cycling may be feasible to impose undrained conditions.

In addition, the vane test could also provide assessment for the residual shear strength, after rotating the blade extensively, whereby the soil along the failure surface becomes remoulded. It is recalled that rotational viscometers (mini-vane) have been used to define the material rheology required when evaluating flow behaviour and shear strength properties of liquefiable materials. Although rotational or cyclic rheometers can provide sound information, it is not clear whether the remoulded strength represents the post-liquefaction residual strength. The low strengths may be a consequence of slip at the boundary along the failure surface and partial drainage may have some influence on the measured brittleness when the material loses strength rapidly, moving from peak to residual.

For loose, non-plastic tailings which have been assessed to have factors of safety greater than 1.0, post-liquefaction strength is assumed as the liquefied undrained shear strength ($S_{u,liq}$). Considering that $S_{u,liq}$ is not replicated in laboratory geotechnical element tests, a simplified approach is to relate $S_{u,liq}$ directly to cone penetration resistance and proportional to the pre-failure

vertical effective stress of a dam (Olson & Stark, 2002; Idriss and Boulanger, 2007; Robertson, 2009; Sadrekarimi, 2014). A lower bound $S_{u,liq}/\sigma_v'$ equal to about 0.04 can be conservatively assumed, and best estimates of values back analysed from case histories are summarized in Table 4 (the peak undrained strength is also presented for comparisons).

Although $S_{u,r}$ is the governing design parameter in post-liquefaction analysis, large uncertainties are associated in assessing this quantity because it is not predicted objectively from measured data.

In low seismicity areas where the factor of safety is greater than 1.0 it is still recommended to assess the reduction in shear strength due to seismic-induced pore pressures to estimate the residual shear strength ($S_{u,r}$). Cyclic direct simple shear (CDSS) tests or cyclic triaxial tests (CTX) in undrained conditions with excess pore pressure measurements are required and, in cases when such tests are not available, correlations established from previous tests may be adopted for preliminary assessment (Marcuson et al., 1990).

Table 4. Peak and liquefied (residual) shear strength

$\frac{S_{u,p}}{\sigma'_{vo}} = 0{,}205 + 0{,}0143\,q_{c1} \pm 0{,}04$	$q_{c1} \leq 6{,}5$ MPa	Olson and Stark (2003):
$\frac{S_{u,liq}}{\sigma'_{vo}} = 0{,}030 + 0{,}0143\,q_{c1} \pm 0{,}03$	Equation (46)	
$\frac{S_{u,liq}}{\sigma'_{vo}} = \frac{0{,}02199 - 0{,}0003124 Q_{tn,cs}}{1 - 0{,}02676 Q_{tn,cs} + 0{,}0001783 (Q_{tn,cs})^2}$ Equation (47)		Robertson (2010)
$\frac{S_{u,liq}}{\sigma'_{vo}} = 0{,}0055\,exp\,(0{,}05 Q_{tn,cs})$ Equation (48)		Jefferies and Been (2016)

6. Conclusion from analysis and design

Design and operation of Tailings Storage Facilities have received considerable attention of mining companies, shareholders, insurers and government agencies after the large-scale devastation and environmental impacts associate to dam failures. The state-of-practice is changing rapidly and critical appraisal of current state of scientific knowledge is being provided by researchers. Important advances in modern practice have been reported in keynote lectures such as the 3rd Mitchell Lecture (Jamiolkowski 2014) describing the geotechnical characterization of the copper tailings at one of the world's largest tailings disposal located at Zelazny Most in Poland. Given the uncertainties that prevail in the geotechnical characterization of tailings, there always exists a probability of localized or catastrophic failure, hence selecting appropriated high factors of safety is justified when assessing both short and long term performance.

Slope stability analysis for drained and undrained loading conditions should be performed and a minimum static factor of safety of 1.5 should be adopted for the condition that yields the coefficient against instability lower limit, routinely called factor of safety. Factors of safety even greater than 1.5 or conservativeness in

parameters assessment could be justified for dams in higher consequences categories and if the materials are very brittle as the values presented in standards and bibliography are minimum values. In this type of approach the peak (yield) strength can be estimated from both *in situ* tests and laboratory tests.

For tailings exhibiting significant softening there are currently uncertainties associated with the residual shear strength and post-seismic reduced shear strength to be used in embankment stability analyses. The critical state strength can be estimated from the state parameter and CSL parameters, instead of the post-liquefaction shear strength from failure case histories which was considered to have very large uncertainties. Fixed residual strength parameters used in limit equilibrium analysis target lower factors of safety within the 1.0 to 1.2 range and cannot take into account progressive failure effects.

For more elaborate and robust design, it is necessary to consider the complete stress–strain behaviour of the soil mass using appropriate constitutive models. In this case, a single general recommendation to assess soil properties is towards a multiparameter analysis combining measurements from laboratory and different *in situ* tests (Schnaid, 2005; Mayne et al, 2009). Laboratory tests carried out on reconstituted samples are the best technique to determine the properties that are invariant with density (in particular the critical friction angle and slope of the CSL) whereas *in situ* tests measure the soil state (state parameter) and ultimate soil conditions (peak effective friction angle, undrained shear strength).

Future research is required in topic areas that are far from being fully resolved:

a) In the design of TSF, the undrained residual shear strength is the governing design parameter for slope stability analy sis under flow instability conditions, whist the peak strength applies for dilative soils. Since the value of S_{ur} is poorly determined, the use of full-flow T-bar and ball penetrometers to measure the residual strength should be stimulated and procedures defining optimized frequency and amplitude displacement cycles should be established.

b) Considerable research has been conducted to examine the instability of tailings that would take place when the deviator stress reaches the peak undrained shear strength (e.g. Sladen et al, 1985; Ishihara, 1993; Lade, 1993). A proper consideration of the *in situ* stress state in respect to the associated peak strength shear envelope is thus essential to evaluate potential instability of tailings. However, the importance of the initial stress anisotropy is often neglected within geotechnical engineering and has been barely addressed in this paper, requiring close consideration in both the design of tailings impoundments and dry stacks.

c) By acknowledging the role of the *in situ* stresses on flow instability, there should be increasing interest in using the self-boring pressuremeter to estimate the geostatic stress ratio K_0. The simplicity of decoding the self-boring pressuremeter curve to obtain the *in situ*

horizontal stress, shear strength and shear stiffness strengthens the need to use this technique in the characterization and design of TSF.

The numerical uncertainty in predicting the behaviour of TSF arises from a combination of several aspects, such as the adequacy of the theoretical models chosen to predict liquefaction, the accuracy of constitutive parameters in describing the material behaviour, the impossibility of reconstructing the deposition process over years or even decades, among other aspects. Predicting soil parameters may be regarded as the primary source of uncertainty in numerical simulations designed to assess triggering likelihood, pushing computational models away from reality and impacting its validation assessment. Utilizing the recent scientific developments descried herein can enhance our ability in predicting liquefaction hazards, especially when the world is experiencing the impacts of climate change, including the increase in precipitation patterns.

Acknowledgments

List of symbols

a	area ratio (=A_N/A_T)
B_q	pore pressure parameter ratio
C_v , C_h	vertical and horizontal coefficients of consolidation
d	probe diameter
e	void ratio
E_{spt}	energy on SPT
F	force
F_d	dynamic reaction force
G	shear modulus
G_o	small strain shear modulus
I_c	soil behaviour type index
I_r	rigidity index
K	hydraulic conductivity
K_o	coefficient of earth pressure at rest
K_D	horizontal stress index
M	slope of critical state line
M_h	hammer mass
N_{kt} , $N_{\Delta u}$	cone factor
N_{spt}	blow count number
p', p	mean and mean effective stress

p_a	atmospheric pressure
q	shear strength
q_t , q_c	measured and correct cone tip resistance
S_u ,	Peak and residual undrained shear strength
t_{50}	time for 50% dissipation of excess pore water pressure
T	Torque
u	pore water pressure
u_o	in situ pore pressure
v	testing rate
Δu	excess pore pressure
λ	slope of critical state line in $e - \ln p$ plot
ν	Poisson's ratio
ψ	state parameter
σ_h , σ'_h	total and effective in situ horizontal stress
σ_{vo} , σ'_{vo}	total and effective vertical stress
ϕ'	effective angle of internal friction
ϕ'_{cs}	critical state angle of internal friction
ϕ'_p	effective peak angle of internal friction
η_1, η_2, η_3	efficiency coefficients
Λ	critical state parameter
Γ	critical state parameter

References

[1] Baligh, M.M (1985) Strain path method. J. Soil Mech. Fdn. Engng. Div., ASCE. 11(7), 1108-1136.

[2] Battaglio M., Jamiolkowski, M., Lancellotta, R. & Maniscalco, R. (1981) Piezometer probe test in cohesive deposits. Cone Penetration Testing and Experience. Proc. Session ASCE National Convention, St Louis, 264-302

[3] Bedin, J., Schnaid, F., da Fonseca, A. V., & Costa Filho, L. D. M. (2012). Gold tailings liquefaction under critical state soil mechanics. Géotechnique, 62(3), 263-267.

[4] Been, K. & Jefferies, M.G. (1985) A state parameter for sands. Géotechnique, 35(2): 99-112.

[5] Been, K.; Jefferies, M.G and Hacheym J.E. (1991). The critical state of sands. Géotechnique, 41(3): 365-381.

[6] Biscontin, G. & Pestana, J.M. (2001) Influence of peripheral velocity on vane shear strength of an artificial clay. Geotech. Testing J., 24(4): 423-429.

[7] Blight, G.E. (1968) A note on field vane testing of silty soils. Can.Geotech. J., 5: 142-149.

[8] Bolton, M.D. (1986) The strength and dilatancy of sands. Géotechnique, 36(1): 65-78.

[9] Burns, S.E. & Mayne, P.W. 1998. Monotonic and dilatory pore-pressure decay during piezocone tests in clay. Can. Geotech. J., 35(6): 1063-1073.

[10] Carrera, A., Coop, M., & Lancellotta, R. (2011) Influence of grading on the mechanical behaviour of Stava tailings. Géotechnique, 61(11): 935-946.

[11] Carter, J.P. (1978) CAMFE, a computer program for the analysis of cavity expansion in soil. Cambridge Univ. Press Dest. of Engng. Report CUEDIC – Soils TR52.

[12] Castro, G. (1969) Liquefaction of sand. Harvard Soil Mechanic Series 87, Harvard University, Cambridge, Massachusetts.

[13] Chandler, R.J. (1988) The In-Situ Measurement of the Undrained Shear Strength of Clays Using the Field Vane," in Vane Shear Strength Testing in Soils: Field and Laboratory Studies, ed. A. Richards (West Conshohocken, PA: ASTM International, 1988), 13-44.

[14] Chandler, R. J., & Tosatti, G. (1995) The Stava tailings dams failure, Italy, July 1985. Proceedings of the ICE-Geotechnical Engineering, 113(2): 67-79.

[15] Chen, S.L. and Abousleiman, N.Y. (2012) Exact undrained elasto-plastic solution for cylindrical cavity expansion in modified Cam Clay soil. . Géotechnique, 62 (5): 447-456

[16] Cho, G., Dodds, J., and Santamarina, (2006) Particle shape effects on packing density, stiffness and strength: natural and crushed sands. J. of Geotech. and Geoenvironmental Engng., 132 (5): 591-602

[17] Collins I.F., Pender, M.J. and Wang, Y. (1992) Cavity expansion in sands under drained loading. Int. J. Numer. Methods Geomech. 16: 3-23.

[18] Coussy, O. (2004) Poromechanics. John Wiley & Sons, Chichester, UK.

[19] Dafalias Y.F. and Manzari M.T. (2004) Simple plasticity sand model accounting for fabric change effects. J. Eng. Mech., ASCE;130(6):622–34.

[20] Dafalias YF, Manzari YF. (2008) SANISAND: simple anisotropic sand plasticity model. Int J. Numer Anal. Methods Geomech.; 32(8): 915–48.

[21] Davies, M.; McRoberts, and E., Martin, T. (2002) Static liquefaction of tailings – Fundamentals and case histories. Tailings Dams.

[22] DeJong, J.T. and Randolph, M.F. (2012) Influence of Partial Consolidation during Cone Penetration on Estimated Soil Behavior Type and Pore Pressure Dissipation Measurements. J. of Geotech. and Geoenviron. Engng, 138 (7): 777-788.

[23] Dienstmann, G., Maghous, S., and Schnaid, F. (2017) Theoretical analysis and finite element simulation for non-linear poroelastic behavior of cylinder expansion in infinite media under transient pore-fluid flow conditions. International Journal of Geomechanics, 17(7): 1-21.

[24] Dienstmann, G., Schnaid, F., Maghous, S. and Dejong, J. (2018) Piezocone penetration rate effects in transient gold tailings. J. Geotech. Geoenviron. Eng. Vol. 144 (2)

[25] Dienstmann, G., de Almeida, F. S., Fayolle, A., Schnaid, F., and Maghous, S. (2018) A simplified approach to transient flow effects induced by rigid cylinder rotation in a porous medium. Computers and Geotechnics, 97: 134-154.

[26] Dormieux, L., Kondo, D., and Ulm, F.J. (2006) Microporomechanics. John Wiley & Sons, Chichester, UK.

[27] Durgunoglu, H. T. and Mitchell, J. K. (1975) Static penetration resistance of soils: I, analysis. Specialty Conf. In Situ Measurement of Soil Properties, Raleigh 1, 151-169.

[28] Forcelini, M., Maghous, S., Dienstmann, G., and Schnaid, F. (2020) Simplified model for interpretation of undrained shear strength from field vane tests in transient soils. J. Geotech. and Geoenvironmental Engng. accepted for publication.

[29] Fourie, A. B., Blight, G. E., & Papageorgiou, G. (2001) Static liquefaction as a possible explanation for the Merriespruit tailings dam failure. Canadian Geotech. J., 38(4): 707-719.

[30] Gens, A., & Alonso, E. E. (2006) Aznalcóllar dam failure. Part 2: Stability conditions and failure mechanism. Géotechnique, 56(3): 185-202.

[31] Hatanaka, M. & Uchida, A. (1996) Empirical correlation between penetration resistance and effective friction angle for sandy soils. Soils Found., 36(4): 1-9.

[32] Hoeg, K., Dyvik, R and Sandbakken, G. (2001) Strength of undisturbed versus reconstituted silt and silty sand specimens. J. Geotech. and Geoenvironmental Engng. 126(7): 606-617.

[33] Idriss, I. M., and Boulanger, R. W. (2004) Semi-empirical procedures for evaluating liquefaction potential during earthquakes, 11th Int. Conf. on Soil Dynamics and 106 Earthquake Engng, and 3rd Int. Conf. on Earthquake Geotech. Engng, D. Doolin et al., eds., Stallion Press, 1: 32–56.

[34] Ishihara, K. (1993) Liquefaction and flow failure during earthquakes. Géotechnique, 43(3): 351-451.

[35] Jamiolkowski, M. (2013) Soil mechanics and the observational methods: challenges at the Zelazny Most tailings disposal facilities. 53rd Rankine Lecture, Geotechnique, 64(8): 590-619.

[36] Jamiolkowski, M. and Masella, A. (2015) Geotechnical characterization of copper tailings at Zelasny Most Site. Keynote Lecture, DMT'15 The 3rd Int. Conf. on the Flat Dilatometer. Marchetti, Monaco & Viana da Fonseca, eds., 25-42.

[37] Jamiolkowski, M.; Ladd, C.C.; Germaine, J.T. & Lancellotta, R. (1985) New developments in field and laboratory testing of soils. State-of-the-Art Report. 11th Int. Conf. Soil Mech. Found. Engng, San Francisco, 4: 57-153.

[38] Jefferies, M.G. and Davies, M.P. (1998) Soil classification by the cone penetration test: Discussion. Canadian Geotech. J., 28(1): 173-176.

[39] Jefferies, M. and Been, K. (2016) Soil Liquefaction – A critical sate approach. Second Edition. CRRC Press, 690p.

[40] Konrad, J.M. (1998) Sand state from cone penetrometer tests: a framework considering grain crushing stress. Géotechnique, 48(2): 201-216

[41] Kim, K., Prezzi, M., Salgado, R. and Lee, W. (2008) Effect of penetration rate on cone penetration resistance in saturated clayey soils. J. of Geotech. and Geoenvironmental Engng. 134 (8): 1142-1153.

[42] Kulhawy, F.H. & Mayne, P.W. (1990) Manual of estimating soil properties for foundation design. Geotech. Engng. Group, Cornell University, Ithaca

[43] Ladanyi, B. & Johnston, G.H. (1974) Behaviour of circular footings and plate anchors embedded in permafrost. Canadian Geotech. J., 11: 531-553.

[44] Ladd, C.C.; Foott. R.; Ishihara, K.; Schlosser, F. & Poulos, H.G. (1997) Stress-deformation and strength characteristics. State-of-the-Art Report. 9th Int. Conf. Soil Mech. Found. Engng, Tokyo, 2: 421-494.

[45] Lade, P. V. (1992) Static instability and liquefaction of loose fine sandy slopes. J. Geotech. Engng, 118(1): 51-71.

[46] Leblanc, C. & Randolph, M. (2008) Geomechanics in the Emerging Social and Technological Age, 12th International Conference on Advances. Indian Institute of Technology, Vol. CD., 822-829

[47] Lerouiel, S. and Hight, D.W. (2003) Behaviour and properties of natural and soft rocks. Characterization and Engng. Properties of Natural Soils. Tan et al Swets & Zeitlinger. 1: 29-254.

[48] Li, W., & Coop, M. R. (2019) The mechanical behaviour of Panzhihua iron tailings. Canadian Geotech. J. 56(3): 420-435.

[49] Li, W., Coop, M. R., Senetakis, K., and Schnaid, F. (2018) The mechanics of a silt-sized gold tailing. *Engng Geology*, 241: 97-108.

[50] Li XS, Wang Y. (1998) Linear representation of steady-state line for sand. *J Geotech Geoenvironmental Engng*, 124(12): 1215–7.

[51] Lo Presti, D.C.F., Jamiolkowski, M., Pallara, O., Cavallaro, A. & Pedroni, S. (1997) Shear modulus and damping of soils. *Géotechnique*, 47(3): 603-617.

[52] Loukidis D, Salgado R. (2009) Modeling sand response using two-surface plasticity. Comput Geotech. 36(1–2):166–86.

[53] Lunne, T.; Robertson, P.K. & Powell, J.J.M. 1997) Cone penetration testing in geotechnical practice, Blackie Academic & Professional, 312p

[54] Mantaras, F.M.B; Odebrecht, E.; Schnaid, F. (2014) On the interpretation of piezocone dissipation testing data. CPT'14; 3rd Int. Symp. on Cone Penetration Testing, Las Vegas, 1: 315-322.

[55] Marchetti, S. (1980) In situ tests by flat dilatometer. J. Geot. Engng. Div. ASCE, 106(3): 299-321.

[56] Marchetti, S. and Totani, G. (1989) Ch evaluation from DMTA dissipation curves. Proc. XII Int. Conf. Soil Mech. Geotech. Engng. Brazil, 1:281-286.

[57] Marchetti, D.; Monaco, P.; Amoroso, S. and Minarelli, L. (2019) In situ tests by Medusa DMT, XVII European Conf. Soil Mech. Geotech. Engng, 1-8.

[58] Marcuson, W.F. et al. (1990). Evaluation and Use of Residual Strength in Seismic Safety Analysis of Embankments. Earthquake Spectra, 6(3):529.

[59] Mayne, P. (2004) In situ soil testing: from mechanics to interpretation. 2nd Int. Conf. on Site Characterization (ISC-2), Portugal.

[60] Mayne, P. (2012) Undisturbed sand strength from seismic cone tests, The Second James K. Mitchell Lecture. Geomechanics and Geoengineering: An International Journal, 1 (4), 239-257

[61] Mayne, P.W. Coop, M.R., Springman, S., Huang, A,B. and Zornberg. A.B. (2009) Geomaterial behavior and testing. State-of-the-Art Report, 17th Int. Conf. Soil Mech. & Geot. Engrg, Alexandria, Egypt. 4: 1-96.

[62] Mitchell, J.K. (1976) Fundamentals of soil behavior, Wiley, New York.

[63] Mitchell, J.K. (2008) Mitigation of liquefaction potential of silty sands. Geotech. Special Publ. No. 180, Research to Practice in Geotech. Engng. Honors Dr. John. H. Schmertmann, ASCE, 433-451.

[64] Mitchell and Soga, (2005) Fundamentals of soil behavior. 3rd ed. :Wiley, New York.

[65] Morgenstern, N.R. (2019) Geotechnical risk, regulation, and public policy. The Sixth Victor de Mello Lecture. Soils and Rocks, 41(2): 107-129.

[66] Morgenstern, N.R., Steven G. Vick, M.; and, Dirk Van Zyl (2015) Report on Mount Polley Tailings Storage Facility Breach, Independent Expert Engineering Investigation and Review Panel, Province of British Columbia.

[67] Niven, E., Robertson, P., Sego, D., and Woeller, D. (2005) On the use of the SPT and CPT in loose sands.Canadian Geotech. Conf, Canadian Geotechnical Society.

[68] Odebrecht, E., Schnaid, F., Rocha, M.M., and Paula Bernardes, G. (2004) Energy efficiency for standard penetration tests. J. of Geotech. and Geoenvironmental Engng. 131 (10), 1252-1263.

[69] Olson, S.M. and Stark, T.D. (2003) Yield Strength Ratio and Liquefaction Analysis of Slopes and Embankments. J. of Geotech. and Geoenvironmental Engng, 129(8): 727-737.

[70] Perlow, M., and Richards, A. F. (1977) Influence of shear velocity on vane shear strength. J. of Geotechnical Engng, 103: 19-32.

[71] Pestana, J.M. and Whittle A. (1999) Formulation of a unified constitutive model for clays and sands. Int. J. Numerical and Analytical Methods in Geomech.; 23:1215-1243..

[72] Peuchen, J., and Mayne, P. (2007) Rate effects in vane shear testing. Offshore site investigation and geotechnics, 1: 11-13.

[73] Plewes H.D., Davis M.P. and Jefferies, M.G. (1992) CPT based screening procedure for evaluating liquefaction susceptibility., Proc. 45th Canadian Geotech. Conf. Canada.

[74] Poulos, S. J. (1981) The steady state of deformation. J. of Geotech. and Geoenvironmental Engng, 107(5), 553-562

[75] Randolph, M. F. (2004) Characterisation of soft sediments for off-shore applications. 2nd Int. Conf. on Site Charact., Milpress, Porto, 1: 209-232.

[76] Randolph, M.F., Low, H. & Zhou, H., (2007) In situ testing for design of pipeline and anchoring systems,

[77] Offshore Site Investigation - Confronting New Challenges and Sharing Knowledge, UK, 251-262.

[78] Randolph, M. F. & Worth, C.P. (1979) An analytical solution for the consolidation around a driven pile. Proc. Int. J. Num. and Anal. Methods in Geomech., 3(3):217-229.

[79] Randolph, M. F. & Hope, S. (2004) Effect of cone velocity on cone resistance and excess pore pressures.

[80] Proc. Int. Symp. on Engng. Practice and Performance of Soft Deposits. Osaka.

[81] Randolph, M. & Andersen, K.H. (2006) Numerical Analysis of T-Bar Penetration in Soft Clay. Int. J. of Geomechanics, 6(6): 411-420

[82] Robertson, P.K. (2010) Estimating in-situ state parameter and friction angle in sandy soils from the CPT. 2nd Int. Symp. on Cone Penetration Testing, CPT'10, USA.

[83] Robertson, P.K. (2010). Evaluation of flow liquefaction and liquefied strength using the cone penetration test. ASCE Journal of Geotechnical and Geoenvironmental Engineering, 136(6), 842-853.

[84] Robertson, P.K. (2012) Interpretation of in-situ tests – some insights. James K. Mitchell Lecture. Proceedings ISC-4 on Geotech. and Geophysical Site Characterization, Brazil. 3-24.

[85] Robertson, P.K. & Campanella, R.G. (1983) Interpretation of cone penetration tests. Canadian Geotechnical J., 20(4): 734-745.

[86] Robertson, P.K.; Campanella, R.G.; Gillespie, D. and By, T. (1988) Excess pore pressure and the flat dilatometer, Proc. Int. Symp. Penetration Testing, Orlando, 1:567-576.

[87] Robertson, P.K.; Wride, C.E.; List, B.R; Atukorala, U.; Biggar, K.; Byrne, W. Campanella, R.G.; Finn, W.D.; Howie, J.A.; Hughes, J. Lord, E.R.F.; Morgenstern, N.R.; Watts, B.D. & Zavodni, Z. (1998) The Canadian Liquefaction Experiment: an overview. Can. Geotech. J., 37(3): 499-504.

[88] Robertson, P.K.; de Melo, L. David; Williams, J.D. and Ward Wilson, G. (2019) Report of the Expert Panel on the Technical Causes of the Failure of Feijão Dam I.

[89] Rowe, P.W. (1963) Stress-dilatancy, earth pressure and slopes. J. Soil Mech. Fdns. Div. ASCE 89, SM3, 37-61.

[90] Sadrekarimi, A. (2014) Effect of soil plastic contraction on static liquefaction triggering analysis., Géotechnique, 64(4): 325-332

[91] Santamarina, J.C. and Cho, G.C. (2004) Soil Behavior: The Role of Particle Shape, Proc. Skempton Conf., London. 6-14.

[92] Santamarina, J. C., Torres-Cruz, L. A., & Bachus, R. C. (2019) Why coal ash and tailings dam disasters occur. Science, 364(6440): 526-528.

[93] Schmertmann, J.H. (1975) Measurement of in situ shear strength. Proc. Specialty Conf. In Situ Measur. of Soil Properties, ASCE, 2, 57-138.

[94] Schmertmann, J.H. (1988) Guidelines for using the CPT, CPTU and Marchetti DMT for geotechnical design. Report FHWA-PA-87-024-84-24, Vol III – DMT Testing Methods and Reduction Data.

[95] Schmertmann, J.H. and Palacios, A. 1979. Energy dynamics of SPT. J. Soil Mech. Fdn. Engng. Div., 105 (8): 909-926.

[96] Schlue, B. F., Moerz, T., and Kreiter, S. (2010) Influence of shear rate on undrained vane shear strength of organic harbor mud. J. of Geotech. and Geoenvironmental Engng, 136: 1437-1447.

[97] Schnaid, F. (2009) In situ testing in geomechanics – The main tests. Taylor & Francis, New York

[98] Schnaid, F. and Houlsby, G.T (1992) Measurement of the properties of sand in a calibration chamber by the cone pressuremeter test. Géotechnique, 42 (4), 587-601.

[99] Schnaid, F. and Yu, H.S. (2007) Interpretation of the seismic cone test in granular soils. Géotechnique, 57 (3): 265-272.

[100] Schnaid, F; Bedin, J.; Viana da Fonseca, A. J. P.; Costa Filho, L. M. (2013) Stiffness and Strength Governing the Static Liquefaction of Tailings. J. Geotech. Geoenvironmental. Engng., 139 (12): 1943-5606.

[101] Schnaid, F., Odebrecht, E., Sosnoski, J. and Robertson, P. K. (2016). Effects of test procedure on flat dilatometer test (DMT) results in intermediate soils. Canadian Geotech. J., 53 (8): 1270-1280.

[102] Schnaid, F., Lourenço, D. and Odebrecht, E. (2017 Interpretation of static and dynamic penetration tests in coarse-grained soils. Géotechnique Letters, 7(2): 113-118.

[103] Schnaid, F.. Belloli, M., Odebrecht, E. and Marchetti, D (2018) Interpretation of the DMT in Silts," Geotechnical Testing J., 41(5): 868-876.

[104] Schnaid, F., Dienstmann, G., Odebrecht, O. and Maghous, S. (2019) A simplified approach to normalisation of piezocone penetration rate effects. Géotechnique, 1-6

[105] Schnaid, F. Marchetti, D. Odebrecht, E. and Belloli, M.V.A. (2020) Medusa DMT in transient silts. Int. Symp. Site Characterization, ISC´6. In press.

[106] Schnaid, F., Nierwinski, H.P. and Odebrecht, E. (2020) Classification and state parameter assessment of granular soils using the seismic cone. J. Geotech. and Geoenvironmental Engng. Accepted for publication.

[107] Schneider, J.A. and Moss, R.E.S. (2011) Linking cyclic stress and cyclic strain based methods for assessment of cyclic liquefaction triggering in sands. Géotechnique Letters, 1: 31-36.

[108] Schneider, J.A. , Lehane, B.M. and Schnaid, F. (2007) Velocity effects on piezocone measurements in normally and over consolidated clays. Int. J. of Physical Modelling in Geotechnics, 7 (2): 23-34.

[109] Seed, H.B. (1979) Soil liquefaction and cyclic mobility evaluation for level ground during earthquakes. J. Geotch. Engng., 105(2): 201-255.

[110] Seed, H.B. (1987) Design problems in soil liquefaction. J. Geotech. Engng. 113(8): 827-845.

[111] Seed, R.B. and Harder, L.F. (1990) SPT-based analysis of cyclic pore pressure generation and undrained residual strength. Proc. H.B Memorial Symp., Berkeley, (2): 351-376.

[112] Seed, H.B., Tokimatsu, K., Harder, L.F., & Chung, R. (1985) Influence of SPT procedures in soil liquefaction resistance evaluations. J. Geotech.l Engng, 111(12):1425-1445.

[113] Senneset, K.; Sandven, R. And Janbu, N. (1982) Evaluation of Soil Parameters from Piezocone Tests. Transport Research Record, 1235: 24-37.

[114] Shuttle, D.A. and Cunning, J. (2007) Liquefaction potential of silts from CPTu. Canadian Geotech. J., 44(1): 1-19.

[115] Skempton, A. W. (1986) Standard penetration test procedures and effects in sands of overburden pressure, relative density, particle size, aging and over consolidation. Géotechnique, 36(3): 425-447.

[116] Silva, M. F., White, D. J. and Bolton, M. D., 2006,"An analytical study of the effect of penetration rate on piezocone tests in clays," Int. J. Analyt. and Num. Meth. Geoemech., 30(6): 501-527.

[117] Suryasentana, S.K. and Lehane, B.M. (2014) Numerical derivation of CPT-based p–y curves for piles in sand, Géotechnique 64(3), 186-194

[118] Suzuki, Y., Lehane, B;M. and Fourie, A. (2014) Effect of penetration rate on piezocone parameters in two silty deposits. Geotech. and Geophysical Characterization 4, Coutinho & Mayne (eds), Taylor & Francis Group. London, 1: 809-815.

[119] Suzuki, Y. and Lehane, B;M. (2014) Rate dependency o qc in two clayey sands, CPT´14 3rd Int. Symp. On Cone Penetration Testing, Ed. Robertson and Cabal, USA, 1: 411-418.

[120] Suzuki Y., Sanematsu, T., and Tokimatsu, K. (1998) Correlation between SPT and seismic CPT." In: Robertson PK, Mayne PW (eds.), Conf. on Geotech. Site Characterization, Balkema, Rotterdam, pp. 1375–380.

[121] Taborda D.M.G., Zdravkovic, L.; Kontoe, S.; and Potts, D.M. (2014) Computational study on the modification of a bouding surface plasticity model for sands. Computers and Geomech., 59: 145-160.

[122] Teh, C.I. & Houlsby, G.T. (1991) An analytical study of the cone penetration test in clay. Géotechnique, 41(1): 17-34.

[123] Torstensson, B. A. (1977) The pore pressure probe. Norsk Jord-Og Fjellteknisk Forbund. Oslo, Foredrag 34.1-34.15. Troedheim, Norway.

[124] Vaid, Y.P., Sivathayalan, S., Uthayakumar, M. and Eliadorani, A. (1995) Liquefaction potential of reconstituted Syncrude sand. 48th Canadian Geotech. Conf., 223-232.

[125] Verdugo, R. and Ishihara, K. (1996) The steady state of sandy soils. Soils & Foundations, 36(2): 81-91

[126] Vesic, A.S. (1972) Expansion of cavities in infinite soil mass. J. of Geotch. Engng. Div., ASCE, 98 (3): 265-290.

[127] Viana Da Fonseca, A., Ferreira. C.M.F., Ramos, C. and Gomez, F.M. (2019) The geotechnical test site in the greater Lisbon area for liquefaction characterisation and sample quality control of cohesionless soils. AIMS Geosciences, 5 (2): 325-343.

[128] Vick, S.G. (1983) Planning, design, and analysis of tailings dams. Wiley Series in Geotechnical Engineering, 365pp.

[129] Weibull, W. (1951) A statistical distribution function of wide applicability. J. Appl. Mech. 18: 293-296.

[130] Wroth, C.P. (1984) The interpretation of in situ soil test. 24th Rankine Lecture. Géotechnique, 34 (4): 449-489.

[131] Wroth, C.P. and Basset, N. (1965) A stress-strain relationship for the shearing behaviour of sand. Géotechnique, 15(1):32-56.

[132] Yu, H.S. (2000) Cavity expansion methods in geomechanics. Kluwer Academic Publishers, UK, 385p.

[133] Yu, H.S. (2004) In situ soil testing: from mechanics to interpretation. 1st James K. Mitchell Lecture. Proceedings ISC-2 on Geotech. and Geophysical Site Characterization, Viana da Fonseca & Mayne (eds.) © 2004 Millpress, 3-38.

[134] Yu, H.S. & Houlsby, G. (1991) Finite cavity expansion in dilatant soils: loading analysis. Géotechnique 41 (2): 173-183.

[135] Yu, H.S. & Mitchell, J.K. (1998) Analysis of cone resistance: a brief review of methods. J. Geotech. And Geoenvironm. Engng., ASCE, 124(2):140-149.

[136] Yu, H.S.; Schnaid, F. & Collins, C. (1996) Analysis of cone pressuremeter tests in sands. J. Geotech. Engng. 122 (8): 623-632

[137] Zhang, Q., Yin Z., Fan, X., Wang, W. and Nie, W. (2015) An experimental study of the mechanical features of layered structures in dam tailings from macroscopic and microscopic points of view. Eng. Geol., 195, 142-154.